Interactive comment on “Tidal variability in the Hong Kong region” by Adam T. Devlin et al.

Anonymous Referee #1

Received and published: 7 December 2018
7 December 2018

Comments on ‘Tidal variability in the Hong Kong region’ by Devlin et al. (OSD)
This paper looks at the variability in the semidiurnal and diurnal tides, and in overtides, around Hong Kong and tries to relate the observed tidal changes to changes over a wider area and in MSL. It is one of a number of papers that have appeared in recent years that have pointed to tantalising associations between changes in tides and MSL that are sometimes enigmatic and always hard to explain. Therefore, the availability of a large data set from a small region such as Hong Kong is to be welcomed. However, as the authors point out, this region has undergone a lot of engineering modifications and it is therefore not the easiest of places to try and separate the impacts on the tides from those modifications from those due to genuine changes in large-scale ocean processes (the NW European coastline is a similarly problematic region given that it has had a lot of dredging etc.). The authors attempt to make that separation by also using data from a small number of sites across the vast area of the South China Sea etc. I found that quite unsatisfactory. The paper seems to me to provide findings which are far from coherent, and so do not lend themselves to easy interpretation. The authors attempt to explain all that diversity by rather (to me) a rambling discussion of ’maybe’ processes such as reclamation, changes in baroclinicity, changes in rivers, resonance shift etc. You can explain anything away in this way.

-Thank you for your review, and for your constructive comments! We are thankful that you recognize that our study is of interest. We are also thankful to have a critical eye to evaluate our results. As we think is clear to you, we attempted to do far too much in this study! We have been studying these tides gauges for quite a while now and have found quite a bit of interesting behaviour that has piqued our curiosity in many ways. In the course of writing this first draft, we tried to include everything that we had observed, even those things that we were not yet quite sure of (such as the “minor tides” tangent that has now been better elucidated to us by the comment of Richard Ray as an error in analysis approach), or things that are hard to make conclusions about (such as trying to determine anything meaningful about the SCS tides relying solely on the sparse and only historical publicly available Mainland China tide gauge network). We admit that we tried to be far too ambitious in this first attempt. Furthermore, this paper has been waiting for review for a very long time, and while we have been waiting, we have moved forward in our work and found new discoveries and methods that have provided new insights about the data in HK. For example, Richard Ray’s comments led us to the correct way to analyse minor tides such as M_3 and N_2 (i.e., use a 9-year window for analyses) which produced stable results without the 9-year “pseudo-cycle” from constituent contamination. However, this focus on minor constituents, while improved, is not very relevant to the overview of tidal correlations in Hong Kong, which is focused on yearly-scale fluctuations that are not as apparent after performing 9-year analyses. This part of the analysis is saved for a future, global-based study of M_3 based on 9-year analyses.

Based on your comments, Richard Ray’s comment, and the new things we have been working on, we have now greatly streamlined this paper and made a better focus on relevant *and communicable results. The major changes are that we have dropped many things in the first draft and made the focus the Hong Kong local results of the four largest tides.*

The relevant omissions are:

- *-The "minor tide" analyses (i.e., N_2, K_2, Q_1, and P_1) and consequently the delta-HAT-8 analyses.*
- *-The South China Sea results and discussion. Also, much of the related introduction materials about the SCS dynamics, internal tide generation and propagation, etc.*
- *-The "historical" vs. "modern "comparisons.*
- *-The later discussion about M_3 and other minor tidal behaviour (this part was erroneous as pointed out by Ray).*
- *-Figures related to the above, which has allowed a better resolution to be used without "tiling" the results and making them too small.*
- *-Removal or downplaying of the suggestion of mechanisms to explain the behaviour, besides some short mentions of the possible importance of engineering projects in HK. This possibility will be explored in an upcoming modelling study using highly accurate DEMs*

-Targeted responses to your individual comments are found below. Many of these comments are not applicable after we removed the majority of things listed above.

-We will do our best to reference our relevant changes in relation to the original text line numbering and sectioning. However, with all the omissions, the form and structure of the text has greatly changed and referring to the old numbering will likely be confusing. Therefore, we will describe the changes in reference to new line numbering where applicable.

"this region has undergone a lot of engineering modifications and it is therefore not the easiest of places to try and separate the impacts on the tides from those modifications from those due to genuine changes in large-scale ocean processes."

-In regard to this comment, in the new version, we have excluded a lot of the hypothesizing about what is causing the tidal changes (i.e., local vs. regional mechanisms) and instead just mention that coastal modifications have had a long history in HK and may be at least partly to blame via possible resonance and frictional changes. And, as we are no longer including or talking about any of the SCS observations, we don't think it is needed to make any substantial hypothesizing about the regional tidal properties.

I read the paper several times and my recommendations are:

(i) to rewrite it to focus only on the local data set from the Hong Kong area which, although may be affected by the engineering changes, does seem to present a reasonably spatially coherent set of findings. And then drop the SCS discussion which is superficial at best for such a large area. A local focus, perhaps with some modelling to provide a sensitivity study, would make for a nice paper.

-Thank you for the feedback and suggestion. We have followed this advice and have now focused only on the Hong Kong results. The SCS discussion has now been omitted, as this data is sparse and historical. Since this dataset is mainly composed of Mainland China observations, which have not been publicly updated since 1997, studying this data does not really reveal anything useful, even though I really hoped that I could have. We had the best of intention in using this data, hoping that a discussion of these results might help fuel an interest in releasing more data publicly, but we admit this case has not been made.

-As to the suggestion about modelling, we decided to not undertake such an endeavor here. It is believed that capturing the full dynamics of the HK waters is a complex question and will take a lot of careful consideration of details (such as highly-accurate DEM that can simulate the differences in tides under different land reclamation projects of the past) and will hopefully be the subject of future studies. This present study is only meant to be an observational study to identify the interesting tidal observations. While we believe that is highly likely that the coastal modifications have something to do with this, it is also believed that proving this via modelling would be worthy of a completely different study, which we do hope to pursue more completely soon.

(ii) focus only the four main constituents. The smaller ones can indeed be mentioned in passing (e.g. if M4 is changing in an opposite way to M2) but it is the main ones that most people are concerned with understanding at the moment and, as Ray has pointed out in his interactive comment, it is not clear that the authors properly understand the variability inherent in some of the minor tides and/or in the software used to determine them. I would also drop figures 7-10.

-Thank you again for the comments which have focused our scope. We do indeed now only discuss the four major constituents (M_2, S_2, K_1, and O_1), and the delta-HAT based on these four tides. The other four major tides (N_2, K_2, P_1, and Q_1) do not add much to the discussion here, and the delta-HATs based on 8 tides was not too much different from the four-tide rendering, so it is better to focus only on the four most stable tides. We have also removed the old versions of Figure 8-10, which were too noisy and mostly useless, and, as illustrated by Ray, are erroneous in approach. However, we have elected to keep Figure 7(now Figure 9) which shows the major tidal anomalies witnessed at Quarry Bay and Tai Po, and now have a briefer discussion about these observations in the context of timing with major reclamation projects as a motivation for future modelling efforts.

(iii) drop the division of the data set into historical/modern. I found the discussion of the differences between the two epochs unconvincing.

-Agreed. We were attempting to make something meaningful out of the sparse Mainland China data in relation to the HK data, but this attempt was unsuccessful. Some brief mentions are still included about the fact that there is an obvious difference in tidal variability in early years and later years at the longer records, which was another reason we decided to keep the (old) Figure 7 (now Figure 9).

(iv) try and not include so many numbers in the text which the reader just cannot absorb.

-Thank you for this comment. We agree that too many numerical results in the text can make a boring "laundry list" of data that is too hard to read. We hope that this issue has now been alleviated by the removal of the SCS data and the historical/modern comparisons.

(v) include some mention of changes in tide gauge operations, aside from just whether they were relocated. For example, are some now using radar gauges instead of float gauges? Have any studies been done of the consequent differences in the tide? Or at least flag this as a possible issue.

-Thank you for this comment. The QB gauge is the only one that was ever re-located, and to the best of our knowledge, there are no known discrepancies or errors have been documented at any gauges. All other gauges have had settlement measurements made since 1991, with no significant changes observed. We have been closely working with the data provider, the Hong Kong Observatory, at the senior level, who are well-versed in the history and quality control of the data and can verify the quality of all of data. All gauges are currently radar gauges. We therefore believe that there are no major datum issues, instrumentation issues, or other errors in our set of data used here. We have also added a few ore publications that are old official reports from HKO about early tidal analyses of the HK tide gauge network.

Some detailed comments:

34 - there is no need for a hyphen in mean sea-level. On the other hand there is in e.g. sea-level rise.

-Thanks for the clarification. We have fixed these instances here and elsewhere.

39 - drop 'inter-tidal'

-Dropped, thanks.

44 - define PSI

-Done

48 - well, if you have chaotic results (which are not necessarily the fault of the authors of course), then you can always explain them as a combination of many processes, especially when you have no real data to back up the suggestions. (I know this is a harsh remark, but that's the way this paper reads to me.)

-Thanks for the comment, and no offense taken. We admit this was a bit rambling. We now have focused this better to be applicable to HK, and only suggest the possibility of the frictional/resonance mechanism under rising MSL because of local engineering changes.

84 - start new sentence at Therefore

-Done.

96 - +/- 5 percent of what?

-This indicates a 5% modification of total sea level due to tides for an arbitrary MSL change. We have tried to make the language clearer.

97 - 65% ditto

-This number is dropped, and the discussion is better focused now.

about 97 - the TAC and delta-HAT acronyms are mentioned here but only explained properly below. It seems to assume the reader has read the other Devlin papers. I would define them a little more fully around here.

-I have tried to explain these metrics better here, or at least enough to be introduced here, with the details better discussed in Methods..

I don't have a problem with the TAC parameter and name by the way, but I really don't like delta-HAT. As I understand it, it reflects the maximum level that would be obtained in a year from the time-dependent amplitudes and phases extracted from the admittance method? But HAT to most people refers to the maximum level that would be obtained by running a set of tidal predictions over 18.6 years. I would find another name for this parameter. Also it has nothing to do with time series as far as I understand it, it is just the sum of the amplitudes for either the 4 or 8 constituents for that year (please clarify if not).

-Thank you so much for this comment. We will try to answer this carefully and explain our logic. Over the course of developing these novel methods in other studies (Devlin et al, 2014; 20171; 2017b), we wrestled with many different acronyms and names for out metrics of what is now TACs and delta-HATs. For instance, originally, we called them TAT (tidal anomaly trends) in Devlin et al., 2014, but later decided that name was inaccurate, as what we observe is not really a "trend". So, we decided that TAC was better later (Devlin et al., 2017). But I felt a little conflicted about changing the acronym, since it had already been established in my previous study. A similar situation applied to the use of delta-HAT. At the onset, my co-authors and I acknowledged that some people would think of the classical definition of HAT (based on the 18.6-year analysis). We decided that using "delta-HAT" would imply a shorter timescale change in this metric, which could not be revealed from an 18.6 yr analysis; we are interested in yearly-scale fluctuations. However, we have always introduced our method as a "proxy" or "indirect estimate" of the change in HAT. Since this language and acronym has been used in a recent paper (Devlin et al., 2017a), as well as in a new paper that studies the Atlantic using these methods which was recently accepted, we really want to keep the language consistent in the current paper about Hong Kong.

To clarify our methods, we do combine the tidal amplitudes and phases of the top four tides garnered from the yearly admittance values into a single complex time series, and the absolute value is taken to show the highest actual level reached by that combination, which is then detrended and regressed against detrended MSL over the same window.

We therefore want to make the case that we want to keep this name of delta-HAT, but we will also better explain the distinction of it being a "proxy" in the manuscript where applicable. If you still take issue with the use of this acronym, we will relent and try to find a new one, especially if you have a good suggestion.

98 - doubled. With respect to what? Any exceedance level will be with respect to a datum.

-Doubled, as in almost double of the exceedance of MSL alone (above an arbitrary datum).

98 - I would drop the TSL acronym. There is no need for too many acronyms. 'Extreme sea level' would do here just as well.

-We have adopted this format now.

176 - tide gauge records

-Fixed.

189 - website should be the website

-Fixed.

213 - this is true only if the nodal and other low-frequency modulations (i.e. perigean) are the same in the real ocean as in the potential. There are many examples from shallow-water areas of them not being the same.

-Good point, and we have added this caveat to the methods. However, every gauge used has been carefully analysed by eye to identify any instances of "leakage" of low-frequency signals (nodal or otherwise). As Ray has instructed in his comment, the 8.85 yr perigean cycle can still be apparent after admittance methods are applied in N_2 and other constituents. But we have now dropped the N_2 analysis from the paper. However, in the HK region, the low-frequency modulations of the four main tides are not apparent after the admittance method is applied.

223 - state these time series are annual values (presumably)

-We have been more explicit in this paragraph about time-series being annual.

226 - reword: which has previously been shown to be more apparent

-Fixed, thanks!

232 - year-to-year change. (See my comment above about delta-HAT which is bad name)

-We have made this change. However, please see the comment above about the use of the delta-HAT name.

234 - typically 75%

-Fixed

237 - you use the word 'minor' here to refer to N2, K2, P1 and Q1, but minor is used for a different set below. I would change 'minor' here to 'latter four' or similar.
about 244 - I would add 'amplitude' many times in here and in the figure captions. For example, you mention 'tidal perturbations' here - perturbations in what? What are

they? I think the problem is the jargon half the time.

-Most of these comments are no longer relevant since I removed a lot of material about minor tides, but I will clarify that we use "tidal perturbations" to indicate the variation of the tidal admittance from the (detrended) mean value.

251-254 - why is this sentence relevant? You don't do any projections into the future.

-This sentence did not mean to assume anything about projections. We include this part to clearly indicate that the calculated TACs can be assumed stable and constant over the time window considered (30 years or less), a "pseudo-linear" assumption, if you will. This point needed to be stressed in previous papers, and this window length was employed in all previous works by Devlin et al. so far. Mainly it is matter of consistency (similar to our justification of keeping the delta-HAT moniker). Comparative analyses in other studies have shown that any longer of a regression analysis may obscure changes in the TAC over time. However, we have modified the text a bit to reflect this explanation, and removed the word "extrapolate" which may have been adding to the confusion.

265 - say why you use the last 30 years. Data better?

-Please see the above comment. To reiterate, longer time window may obscure changes in the TAC values, and 30 years has been shown to be a good window to use based on previous studies.

273 - you use the words historical/modern here and early/later lower down which gets confusing. Anyway, as mentioned above, I would drop this aspect.

-These comments should no longer be applicable, as the historical and minor material has been omitted now.

293 - does 'minor' here mean the 4 above? Be clear.

- These comments should no longer be applicable

304 - I am not sure anyone knows where Beibu Gulf is (no offence intended). Perhaps add 'on the south coast of China'.

-Some in America and the Western world would know it as the Gulf of Tonkin. I was trying to use the name that the locals use. However, this comment is now moot since I have removed the SCS discussions.

306/308 - now we have early/later

-No longer included.

325 - you quantify the others but not for Bintulu.

-No longer relevant.

392 - a record can be flat or have zero trend. You can't have a 'flat trend'

-Fixed.

413 - 'minor' here means quite a different set (discussed by Ray)

-No longer relevant.

417 - there is discussion of the perigean dependence of N2 along the China coast in the Feng et al. paper by the way.

-Thanks for the reference. This is no longer relevant to the current paper, but I am doing a new study about the perigean-modified tides based on a world-wide set of data using 9-year analyses, so I will read that paper with great interest!

423 - 'missed'. It looks to me to be there is a little bit.

-No longer relevant; material removed.

425 - why is this interesting? N2 would be in phase wouldn't it in a small area like this?

-No longer relevant; material removed.

456 - 'it is apparent'. It is in figures 7 and 8 ok but not to me for 9 and 10?

-No longer relevant; material removed.

464 - who –> which

-No longer relevant; material removed.

467 - will be –> are

-No longer relevant; material removed.

470 - correlations of what?

-No longer relevant; material removed.

659 - the Conclusions for the reasons for the tidal changes are just speculation. You should start this section by reviewing what the data tells you.

-Thanks for this comment. We have done a lot of work to rewrite the conclusion section with some more focus. We now try to simply discuss the observations, discus lightly some possible reasons (i.e., harbour changes or regional climate changes), and lay out some future possible steps.

824 - it is hard to see the red and green on top of the dark blue. The caption should say the blue shows depth in metres.

-No longer relevant; maps of the SCS are now removed.

figure 3 and others - I read this paper on A4 paper and I cannot read what’s in the legends or even the axis annotations of some of the figures.

-Figure have all ben redone in the new version. Without the SCS material, we now use single-panel figures, focusing only on the most relevant observations.

In (b) and (d) there is a red square box for the Hong Kong area not mentioned in the caption. They also have the Egbert model values which are not discussed in the text, so why have them?

-No longer relevant; material removed.

In (c) there are captions for each point like CHC which are unnecessary given Figure 1.

-OK, we now only show station names in Figure 1, and all other figures have names removed.

figure 5 etc. caption - again the word ’amplitude’ needs adding whenever you say something like ’detrended (M2+S2+K1+O1)’.

-Thanks, fixed!

figure 7 - I can understand the mean values for the tides but the mean values of MSL require to know the datum.

-All water levels given for MSL are in relation to the “chart datum” as defined by the Hong Kong Observatory. The chart datum is defined as an additional 0.146 m below the Hong Kong Principal Datum (HKPD). The HKPD determined for the years 1965-1983 was approximately 1.23 m below MSL. The HKPD has been recently re-determined using data from 1997-2015 to be 1.30 m below MSL. Therefore, all MSL values are given in relation to the sum of both values, so 1.376 m for the early years, and 1.446 m for the later years (approximately). Please see the following weblink for a full history of the datum in HK: https://www.hko.gov.hk/blog/en/archives/00000204.htm. However it should be mentioned that what is shown in current figure, what is plotted for the MSL component is the zero-frequency component of the harmonic analysis (i.e., de-tide MSL) which may have some offset from the full MSL (tides included) as determined from HKO. We now include more material about this history in the text.

figure 9 and 10 - I can’t read the information on the right.

-No longer relevant; material removed.

Table 1 - add an extra column for the number of years of data used.

-OK, done!

Interactive comment on "Tidal variability in the Hong Kong region" by Adam T. Devlin et al.
Anonymous Referee #2
Received and published: 3 January 2019

The authors set out to investigate how the observed tides around Hong Kong, and in the wider SCS, have changed over the last decades. The use of such a large data set from a small region is interesting, and there are some intriguing results, but there are issues I think must be addressed before this could be published. Both of these points are already raised by Review 1 and by Richard Ray in their comments, and I second them here (hence the brevity of this review).

-Thank you for your overview and gentle review. We have worked hard in this revision to make some major changes, based on the very helpful comments of Reviewer #1 and the additional helpful comments and explanations added by Richard Ray. It has also been a long time since our initial submission of this paper (we were waiting for an initial review for over 6 months), and a lot of new work and new discoveries are evolving in our examination of the HK waters.

In this version, we have removed a lot of the contentious material. We now only use the four major tidal constituents and the sum of the four as the delta-HAT. We also remove the overtide analyses, the SCS analyses and discussion, and the historical/modern comparisons. Finally, we have removed the "minor tide" discussion of the M_3 *tide and other lesser components, because, as pointed out by Ray, this effort was somewhat flawed in execution. Richard's comments were quite helpful in elucidating the proper method of analysing perigee-influenced tides (such as* M_3 *and* N_2*), in that a 9-year analysis window should be employed. In fact, we are moving forward in a new study to examine the global occurrence of the* M_3 *tide using 9-year analysis windows, and these results are quite interesting, including the HK results. However, these results are now not as relevant to the current study, so all previous material about this has been removed. We now focus only on the local HK results, and downplay talking too much about the mechanisms why, though it is still hypothesized that the local harbor changes are likely part of the answer. However, regional SCS changes under climate change may also be a factor, and, as Reviewer #1 points out, it is difficult to separate the local engineering changes from regional climatic changes. Therefore, we try not to suppose or speculate too much here, mainly we just report what is observed. We do intend to design a new modelling study in the near future that will employ a highly-accurate DEM of HK and apply some of the historical coastal changes to examine if tidal properties can be affected by such changes, and we mention this intention for the future in the new manuscript. Please also see our complete responses to Reviewer #1 for additional responses and explanations.*

The relevant omissions are:

- *-The "minor tide" analyses (i.e.,* N_2*,* K_2*,* Q_1*, and* P_1*) and consequently the delta-HAT-8 analyses.*
- *-The South China Sea results and discussion. Also, much of the related introduction materials about the SCS dynamics, internal tide generation and propagation, etc.*
- *-The "historical" vs. "modern "comparisons.*
- *-The later discussion about M3 and very minor tidal behaviour (this part was erroneous as pointed out by Ray).*
- *-Figures related to the above, which has allowed a better resolution to be used without "tiling" the results and making them too small.*

-Removal or downplaying of the suggestion of mechanisms to explain the behaviour, besides some short mentions of the possible importance of engineering projects in HK. This possibility will be explored in an upcoming modelling study using highly accurate DEMs

Major comments:

The paper is a difficult read, mainly because we are constantly interrupted by quantifications. The reader could look up numbers in the figures and tables rather than being told that this gauge changed this much compared to that gauge. Maybe consider saying that "A increased more than B with a factor N".

-Thank you for the comments. We agree that the previous version was a bit confusing and had too many numbers to talk about. We hope that most of these concerns will have been alleviated by the removal of the SCS material, the minor tides, and the historical/modern comps. Beyond this, we have rewritten the remainder of the paper with a careful eye on giving a smooth dialogue without too many quantification interruptions.

The overtide analysis really doesn't add much, even if it wasn't flawed (see Ray's comment). If it is to be included, and I don't think it will be significant once it is analysed properly, we will have to be told why the changes are of interest. I think it would be more worthwhile, and this is seconding Review 1, to focus on the main constituents around Hong Kong alone, and delete the speculations about why the tides may have changed in the SCS. If the latter part is to be included, we need to be told with more certainty why these changes have occurred.

Thank you once again. We agree and have now removed the overtide discussion. We now focus only on the largest and most familiar four tides and have downplayed most of the discussion that speculates about the reasons why. As mentioned above, we do hypothesize that the harbour changes may be at play, but without any modelling or better explanations (which may be available after future studies are completed), it is difficult to explain the relative importance of local and regional changes to changing tides.

Minor comments:

L127: it is surprising to not see references to work by Alford and collaborators here.

-Thanks for the suggestion. We did in fact read some of Alford's papers and did have some references included in earlier versions of the manuscript. However, we edited many times and removed a lot of this discussion that was determined to not be as relevant to the new direction of the manuscript and had somehow removed a few papers that were done by Alford and other collaborators in the text, though they are still listed in the Reference list (e.g., Alford, 2008; Chinn et al., 2012). We have re-evaluated these sections, and now cite these two papers in the appropriate place now.

L176-196: I suggest deleting this and just give a very brief summary: we have NN gauges spanning NN years (see table and figures: : :).

-Thanks, we have now honed down this section to be brief according to your suggestion.

L273: why distinguish between historical and modern, using some arbitrary cutoff? Technically, they are all historical, since they are in the past.

-Thanks for the comment. We agree and have removed the comparisons of historical/modern times.

Tidal variability in the Hong Kong region

Adam T. Devlin
Department of Geography and the Environment, Jiangxi Normal University.
Nanchang, Jiangxi, China
Institute of Space and Earth Information Science, The Chinese University of Hong Kong, Shatin,
Hong Kong SAR, China
Shenzhen Research Institute, The Chinese University of Hong Kong, Shenzhen, Guangdong, China

Jiayi Pan*
Institute of Space and Earth Information Science, The Chinese University of Hong Kong, Shatin,
Hong Kong SAR, China
Department of Geography and the Environment, Jiangxi Normal University.
Nanchang, Jiangxi, China
Shenzhen Research Institute, The Chinese University of Hong Kong, Shenzhen, Guangdong, China

Hui Lin
Institute of Space and Earth Information Science, The Chinese University of Hong Kong, Shatin,
Hong Kong SAR, China
Department of Geography and the Environment, Jiangxi Normal University.
Nanchang, Jiangxi, China

* - Corresponding author

Re-submitted to *Ocean Science*

March 2019

Abstract

Mean sea level (MSL) is rising worldwide, and correlated changes in ocean tides are also occurring. This combination may influence future extreme sea levels, possibly increasing coastal inundation and nuisance flooding events in sensitive regions. Analyses of a set of tide gauges in Hong Kong reveal complex tidal behavior. Most prominent in the results are strong correlations of MSL variability to tidal variability; these tidal anomaly correlations (TACs) express the sensitivity of tidal amplitudes and phases (M_2, S_2, K_1, O_1) to MSL fluctuations and are widely observed across the Hong Kong region. At a few important harbor locations, combined tidal variability that can approximate changes in the highest astronomical tide (δ-HAT) is highly sensitive to MSL variability which may further increase local flood levels under future MSL rise. Other open-water locations in Hong Kong only show TACs for some individual tides but not for combined tidal amplitudes, suggesting that the dynamics in enclosed harbor areas may be partially frequency-dependent and related to resonance or frictional changes. We also observe positive correlations of the fluctuations of diurnal (D_1) tides to semidiurnal (D_2) tides at most locations in the region which may lead to further amplified tidal ranges under MSL. Overall, it is shown that tidal changes in the Hong Kong coastal waters may be as important as MSL rise in impacting future total water levels.

1. Introduction

Ocean tides have long been thought of as a stationary process, as they are driven by the gravitational forcing of the Sun and Moon whose motions are complex but highly predictable (Cartwright and Tayler, 1971). Yet, long-term changes in the tides have been observed recently on regional (Ray, 2006; Jay et al., 2009; Zaron and Jay, 2014; Rasheed and Chua, 2014; Feng et al., 2015; Ross et al., 2017) and worldwide spatial scales (Woodworth, 2010; Müller, et al. 2011; Haigh et al., 2014; Mawdsley et al., 2015), concurrent with long-term global mean sea level (MSL) rise (Church and White, 2006; 2011). Since gravitational changes are not the reason, the tidal changes are likely related to terrestrial factors such as changes in water depth which can alter friction (Arbic et al, 2009), coastal morphology and resonance changes of harbor regions (Cartwright, 1972; Bowen and Gray, 1972; Amin, 1983; Vellinga et al., 2014; Jay et al., 2011; Chernetsky et al., 2010, Familkhalili & Talke, 2016), or stratification changes induced by increased upper-ocean warming (Domingues et al., 2008; Colosi and Munk, 2006; Müller, 2012; Müller et al., 2012), all of which are also related to sea-level rise.

Tides can also exhibit short-term variability correlated to short-term fluctuations in MSL (Devlin et al., 2014; 2017a; 2017b). These variabilities may influence extreme water level events, such as storm surge or nuisance flooding (Sweet and Park, 2014; Cherqui et al., 2015; Moftakhari et al., 2015; 2017; Ray and Foster, 2016; Buchanan et al., 2017). Such short-term extreme events are obscured when only considering long-term linear trends. Any significant additional positive correlation between tides and sea-level fluctuations may amplify this variability and implies that flood risk based only on the superposition of present-day tides and surge onto a higher baseline sea-level will be inaccurate in many situations. The analysis of the correlations between tides and sea level at a local or regional scale can indicate locations where tidal evolution should be considered a substantial modification to sea-level rise. Moreover, since storm surge is a long wave, factors affecting tides can also alter storm surge (Familkhalil and Talke, 2016; Arns et al., 2017). Hong Kong is often subject to typhoons, with some recent storms yielding anomalously high storm surges, so this issue is of critical interest.

Recent works surveyed tidal anomaly correlations (TACs) at multiple locations in the Pacific, a metric that quantifies the sensitivity of tides to short-term sea-level fluctuations (Devlin et al., 2014; Devlin et al., 2017a), finding that over 90% of tide gauges analyzed exhibited some measure of correlation in at least one tidal component. In a related work (Devlin et al., 2017b), the combined TACs of the four largest tidal components was calculated as a proxy for the changes in the highest astronomical tide (δ-HAT), with 35% of gauges surveyed exhibiting a sensitivity of δ-HATs to sea-level fluctuations of at least ± 50 mm under a 1-m sea-level change (~5%). A recent paper performed similar analyses in the Atlantic Ocean, finding comparable results to the Pacific (Devlin et al., 2019). The greatest δ-HAT response in the global ocean is seen in Hong Kong (+ 650 mmm^{-1}). A probability distribution function analysis revealed that an extreme sea level exceedance which includes tidal changes can be nearly double (+150 mm) that which only considers MSL exceedance alone (+78 mm) over the past 50 years (Devlin et al., 2017b). This demonstrates that the non-stationarity of tides can be a significant contributor to total water levels in this region and warrants closer examination.

Hong Kong and the Pearl River Delta (PRD) region contains many densely-populated urban metropolises with extensive coastal infrastructure and extensive recent land reclamation projects. Sea-level rise in the region has exhibited a variable rate in the region over the past 50 years (Li and Mok, 2012; Ip and Wai, 1990), but a common feature of all sea level records in the SCS is a steep increase in the late 1990s with a subsequent decrease in the early 2000s, followed by a sustained increase to the present day. In addition to this variable MSL behavior, there are also anomalous tidal events observed at gauges in semi-enclosed harbor regions during the late 1990s and early 2000s (shown and discussed below), corresponding to times of both rapidly changing sea level and aggressive land reclamation.

In this study, we document the fine-scale variability of tidal behavior and variability in the Hong Kong waters in response to MSL variability by performing a spatial and temporal analysis of tidal sensitivity to MSL variations in Hong Kong using the tidal anomaly correlation (TAC) method at 12 closely-located tide gauges.

2. Methods

2.1 Data sources

A set of 12 tide gauge records in the Hong Kong region were provided by the Hong Kong Observatory (HKO) and the Hong Kong Marine Department (HKMD), spanning from 12 to 65 years in length, including two gauges that are “historical” (i.e., no longer operational). The longest record is the North Point/Quarry Bay (QB) tide gauge, located in Victoria Harbor, established in 1954 and relocated from North Point to Quarry Bay in 1986.

The datums were adjusted and quality controlled by HKO to provide a continuous record (Ip and Wai, 1990). Another long and continuous record is located at Tai Po Kau (TPK) inside Tolo Harbor. Gauge locations in Hong Kong are shown in Figure 1, with the gauges from HKO indicated by green markers, gauges from HKMD by light blue, and historical (non-operational) gauges by red. Figure 2 shows the environment of the South China Sea, with the location of Hong Kong indicated by the red box. Table 1 lists the metadata for all locations, including latitude, longitude, overall record length, and data used in this study.

2.2 Tidal admittance calculations

Our investigations of tidal behavior use a tidal admittance method. An admittance is the unitless ratio of an observed tidal constituent to the corresponding tidal constituent in the astronomical tide generating force expressed as a potential, *V*, divided by the acceleration due to gravity, *g*, to yield $Z_{pot}(t) = V/g$, with units of length that can be compared to tidal elevations, $Z_{obs}(t)$, via harmonic analysis. Yearly harmonic analyses are performed on both $Z_{obs}(t)$ and $Z_{pot}(t)$ at each location, using the R_T_TIDE package for MATLAB (Leffler and Jay, 2009), a robust analysis suite based on T_TIDE (Pawlowicz, 2002). Nodal and other low-frequency astronomical variabilities are typically present with similar strengths in both the observed tidal record and in $Z_{pot}(t)$, but their effects are mostly eliminated in yearly analyzed admittance time series. This may not always hold true in shallow-water areas but does seem to valid for the locations and tides analyzed in Hong Kong. The tidal potential is determined based on the methods of Cartwright and Tayler (1971). The result from a single harmonic analysis of $Z_{obs}(t)$ or $Z_{pot}(t)$ determines an amplitude, *A*, and phase, *θ*, at the central time of the analysis window for each tidal constituent, with error estimates. A moving analysis window produces an annual time-series of amplitude, $A(t)$, and phase, $\theta(t)$, with the complex amplitude, $\mathbf{Z}(t)$, given by:

$$\mathbf{Z}(t) = A(t)e^{i\theta(t)} \quad (1)$$

The tidal admittance (**A**) and phase lag (**P**) are formed using Eqs. (2) and (3)

$$\mathbf{A}(t) = abs\left|\frac{\mathbf{Z}_{obs}(t)}{\mathbf{Z}_{pot}(t)}\right|, \quad (2)$$

$$\mathbf{P}(t) = \theta_{obs}(t) - \theta_{pot}(t) \quad (3)$$

The harmonic analysis procedure also provides an annual MSL time-series. For each resultant dataset (MSL, **A** and **P**), the mean and trend are removed from the time series to allow direct comparison of their co-variability. The magnitude of the long-term trends is typically much less than the magnitude of the short-term variability, which has previously been shown to be more apparent (Devlin et al., 2017a; 2017b).

Tidal sensitivity to sea-level fluctuations is quantified using tidal anomaly correlations (TACs), the relationships of detrended tidal variability to detrended MSL variability. We determine the sensitivity of the amplitude and phase of individual constituents (M_2, S_2, K_1, O_1) to sea-level perturbations at the yearly-analyzed scale. We also consider a proxy for the change in the highest astronomical tide (δ-HAT) by combining the yearly analyzed time series of the four largest tidal amplitudes (M_2, S_2, K_1, and O_1), typically ~75% of the full tidal range (δ-HAT). The detrended time series of the year-to-year change of the δ-HATs are compared to detrended yearly MSL variability in an identical manner as the TACs, and both are expressed in units of millimeter change in tidal amplitude per 1-meter fluctuation in sea-level (mmm^{-1}). These units are adopted for convenience, though in practice, the observed fluctuations in MSL are on the order of ~ 0.25 m. The phase TACs are reported in units of degree change per 1-meter fluctuation in sea-level. The TAC methodology can also be used to examine correlations between different parts of the tidal spectrum. We additionally examine the sensitivity of combined diurnal (D_1; $K_1 + O_1$) tidal amplitudes to semidiurnal (D_2; $M_2 + S_2$) tidal amplitudes (D_1/D_2 TACs). The units of the D_1/D_2 TACs are dimensionless (i.e., mm/mm), and statistics are calculated as above.

The definition of the year window used for harmonic analysis may have an influence on the value of the TAC or δ-HAT, e.g. calendar year (Jan-Dec) vs. water year (Oct-Sep). To provide a better estimate of the overall correlations for all data we take a set of determinations of the correlations using twelve distinct year definitions (i.e., one-year windows running from Jan-Dec, Feb-Jan, …, Dec-Jan.). We take the average of the set of significant determinations (i.e., p-values of < 0.05) as the magnitude of the TAC or δ-HAT. For an estimate of the confidence interval of the TAC or δ-HAT, the interquartile range (middle 50% of the set) is used. A step-by-step description of the TAC and δ-HAT methods, including the details of the calculations of the regressions and statistics can be found in the supplementary materials of Devlin et al. (2017b). For the very long record stations (e.g., QB and TPK), we only consider the past 30 years for TAC and δ-HAT determinations. Comparative analyses in other studies have shown that any longer of a regression analysis may obscure changes in the TAC over time, so using the past 30 years is a good window that standardizes results with the rest of the Hong Kong tide gauge networks, which are typically

~12-30 years long. Finally, we highlight some anomalous tidal events observed at certain Hong Kong gauges, and discuss the temporal evolution of the tidal characteristics in Hong Kong.

3. Results

The individual TACs for amplitude and phase in Hong Kong are discussed first, followed by the δ-HATs and the D_1/D_2 TACs. In all figures, significant positive results will be reported by red markers, significant negative results by blue markers, and insignificant values are shown as black markers. The relative size of the markers will indicate the relative magnitude of the TAC or δ-HAT according the legend scale on each plot. All numerical results for the major amplitude TACs (M_2, S_2, K_1, and O_1) are listed in Table 2, and the δ-HATs and D_1/D_2 TACs are listed in Table 3. Phase TACs of the individual constituents are reported in Table S1 of the supplement.

3.1 Tidal anomaly correlations (TACs)

The strongest positive M_2 TACs are seen at Quarry Bay (+218 ± 37 mm m^{-1}), and at Tai Po Kau (+267 ± 42 mm m^{-1}), with a smaller positive TAC seen at Shek Pik (Figure 3). In the waters west of Victoria Harbor, all gauges except Kwai Chung exhibit moderate negative TACs. The semidiurnal phase TACs in Hong Kong (shown in the Supplementary materials, Figure S1) show an earlier M_2 tide under higher MSL at QB and TPK and a later tide west of Victoria Harbor. The S_2 results in Hong Kong (Figure 4) show that only QB and TPK have significant amplitude TAC values (though smaller than M_2), and the S_2 phase TACs in Hong Kong (Figure S2) also show an earlier tide at QB and TPK under higher MSL.

The diurnal TACs in Hong Kong generally exhibit a larger-magnitude and more spatially-coherent response than semidiurnal TACs. Like M_2, the strongest K_1 values in Hong Kong (Fig 5) are seen at QB (+220 ± 15 mm m^{-1}) and TPK (+190 ± 68 mm m^{-1}). The O_1 results in Hong Kong (Fig 6) are like the M_2 results, showing positive TACs at QB (+146 ± 11 mm m^{-1}) and TPK (+100 ± 25 mm m^{-1}), and strongly negative TACs west of QB. However, unlike the semidiurnal constituents, the phase TACs for K_1 are mostly insignificant in Hong Kong (Figure S3), and O_1 phase TACs (Figure S4) are only significant at QB.

3.2 Combined tidal variability and tidal co-variability

The TACs are widely observed in Hong Kong, but the δ-HATs are only of significance at discrete locations (Figure 7). In Hong Kong, five stations exhibit significant δ-

HAT values, with QB and TPK having very large positive magnitudes (+665 ± 85 mm m^{-1} and +612 ± 210 mm m^{-1}, respectively), and Shek Pik having a lesser magnitude of +138 ± 47 mm m^{-1}. Conversely, Ma Wan and Chi Ma Wan exhibit moderate negative δ-HAT values, (~ -100 mm m^{-1}). The remainder of gauges (which are mainly open-water locations) have statistically insignificant results for the combined tidal amplitudes, even where some large individual TACs were observed. This shows that the combined tidal amplitude effect as expressed by the δ-HATs is most important in semi-enclosed harbors. The D_1/D_2 TACs are also important in Hong Kong and are seen at almost every location. All significant D_1/D_2 TACs results are positive (Figure 8), and at most locations the correspondence is nearly 1-to-1, indicating that a change in D_1 can yield a nearly-identical magnitude change in D_2, and vice-versa. Smaller magnitude relations are seen in the western areas of the HK region.

3.3 Anomalous tidal events at Hong Kong harbor locations

The overall temporal behavior of the tidal spectrum at enclosed harbor locations in Hong Kong (Quarry Bay and Tai Po Kau) is especially interesting, and we report here what is observed. In Figure 9, the time series of water level spectrum components are shown for QB and TPK, presenting the D_1 (K_1 + O_1) band (a), the D_2 (M_2 + S_2) band (b), the OT (M_4 + M_6 + MK_3 + MO_3 + MS_4 + MN_4 + SN_4) band (c) and mean sea-level (MSL) (d), given as normalized amplitudes with mean values shown in the legends. The magnitude of MSL is given in relation to the Hong Kong Chart Datum as defined by the Hong Kong Observatory. The Chart Datum is defined as an additional 0.146 m below the Hong Kong Principal Datum (HKPD). The HKPD determined for the years 1965-1983 was approximately 1.23 m below MSL. The HKPD has been recently re-determined using data from 1997-2015 to be 1.30 m below MSL. Therefore, all MSL values are given in relation to the sum of both values, so 1.376 m for the early years, and 1.446 m for the later years (www.hko.gov.hk).

Some very notable features of the tides are clear. At QB, the early part of the record shows nearly constant tidal amplitudes in D_1, while D_2 amplitudes show a slight decrease, and MSL exhibits a slight positive trend. In the late 1980s, however, both D_1 and D_2 increase drastically until around the year 2003, at which time both tidal bands undergo a rapid decrease of amplitude of ~15%, sustaining this diminished magnitude for about five years before increasing nearly as rapidly. The OT band shows a sustained increase over the historical record, but many of the fluctuations around the trend are anti-correlated to the perturbations in D_1 and D_2, and during the times of diminished major tides, the OTs increase by about +20%. The MSL record is also highly variable at QB, with a nearly zero trend during the increase in tides seen in the 1980s, followed by a strong increase from ~1993-2000, and then a steep decrease concurrent with the time of diminished tides before increasing again. The gauge at TPK shows a similar tidal behavior, though the timing and magnitudes are different. The increase in D_1 and D_2 at TPK in the 1980s is much larger and peaks earlier than QB, reaching a maximum around 1996, and then decreasing around 1998, about five years before the drop at QB. Both locations experience an absolute minimum around 2007 in D_2, but the D_1 minimum at TPK leads the QB minimum by a few years. These observed anomalies are only observed at these two gauges; other locations in Hong Kong did not reveal similar behavior.

4. Discussion

4.1 Summary of observed tidal variability

This survey has identified several types of tidal variability in Hong Kong. The TACs of individual tides are present at many Hong Kong locations, while the δ-HATs appear to be more locally important, as the strongest responses are mainly concentrated at specific locations (e.g., QB and TPK). The M_2 response (Fig 3) is negative at gauges just west of Quarry Bay and positive at Shek Pik, with a similar pattern seen for the O_1 TACs (Fig 6). Conversely, the K_1 TAC results are generally positive (Fig 5). At both QB and TPK, the positive reinforcements of individual tidal fluctuations lead to very large δ-HATs, though moderately negative δ-HATs are seen near QB at CMW and MW (Fig 7). The spatial connections in the semi-enclosed center harbor regions suggest a connected mechanism; this area is where most recent Hong Kong coastal reclamation projects have occurred, including the construction of a new island for an airport, shipping channel deepening and other coastal morphology changes. Such changes in water depth and coastal geometry strongly suggest a relation to frictional or resonance mechanisms.

The D_1/D_2 TAC relations (Fig 8) are a more regionally-relevant phenomenon, being significant nearly everywhere in Hong Kong. The majority of significant D_1/D_2 TACs are positive, with most being nearly 1-to-1 (i.e., a ~1-mm change in D_1 will yield a ~1-mm change in D_2), confirmed by the close similarity of temporal tidal trends of the D_1 and D_2 tidal bands in Hong Kong (Fig 9). This aspect of tidal variability in Hong Kong may be related to the dynamics near the Luzon Strait, where large amounts of baroclinic conversion in both D_1 and D_2 tides may tend to couple the variabilities (Jan et al., 2007; 2008; Lien et al., 2015; Xie et al., 2008; 2011; 2013). The D_1 and D_2 internal tides may interact with each other as well as with other frequencies, such as the local inertial frequency, *f*, via parametric subharmonic instability (PSI) interactions (McComas and Bretherton, 1977; MacKinnon and Winters, 2005; Alford, 2008; Chinn et al., 2012), a form of resonant triad interactions (Craik, 1985). The low-mode baroclinic energy can travel great distances, being enhanced upon arrival at the shelf and leading to the further generation of baroclinic energy. In the western part of Hong Kong, the D_1/D_2 relationships are less than 1 to 1 (~0.33 to ~0.25 at TBT and LOP, respectively). This may be partially influenced by effects of the Pearl River, which discharges part of its flow along the Lantau Channel. The flow of the river is highly seasonal and ejects a freshwater plume at every ebb tide that varies by prevailing wind conditions and by the spring-neap cycle (Pan et al, 2014). The plumes may affect turbulence and mixing in the region and can dissipate energy away the tidal bands, which may "decouple" the correlated response of D_1 and D_2 seen in the rest of the Hong Kong coastal waters.

4.2 Effects of local dynamics on tidal variability

Hong Kong has had a long history of land reclamation to accommodate an ever-growing infrastructure and population, including the building of a new airport island (Chep Lap Kok), new land connections, channel deepening to accommodate container terminals, and many bridges, tunnels, and "new cities", built on reclaimed land. All of these may have changed the resonance and/or frictional properties of the region. Tai Po Kau has also had some land reclamation projects that have changed the coastal morphology and may have modulated the tidal response. Both locations also show coherent D_1/D_2 TACs, as well as having the largest positive δ-HATs, and large tidal anomalies (Figure 9). Other locations in Hong Kong did not show such extreme variations, so these variations appear to only be amplified in harbor areas. Decreases in friction associated with sea-level rise may lead to higher forcing tides, and those changes may also be amplified by the close correlations of D_1 and D_2 variability or local harbor development which may further decrease local friction. Hence, a small change in friction due to a small sea-level change may induce a significant change in tidal amplitudes. The positive reinforcement of multiple tides correlated with regional sea-level adjustments may amplify the risks of coastal inundation and coastal flooding, as evidenced by the gauges that had the largest δ-HAT values.

4.3 Limitations of this study and future steps

The inventory of tide gauges in Hong Kong revealed new dynamics and spatial connections in the area. However, some gauges are of short length and/or riddled with data gaps, making a full analysis of the area problematic. For example, the Tsim Bei Tsui (TBT) gauge covers a long period, but there are significant gaps in the record, which complicated our analysis. This gauge is located within a harbor region (Deep Bay), bordered to the north by Shenzhen, PRC, which has also grown and developed its coastal infrastructure in past decades, therefore, one might expect similar dynamics are was seen at QB and TPK. While there were moderately significant D_1/D_2 correlations at TBT, no significant TACs or δ-HATs were observed. The large anomalies seen at QB and TPK around 2000 are suggested by the data at TBT, but some data is missing around this time, making any conclusions speculative. The Deep Bay region is ecologically sensitive, being populated by extensive mangrove forests which may be disturbed by rapidly changing sea levels (Zhang et al., 2018), so accurate determination of future sea-levels is of utmost importance to the vitality of these important ecosystems. Future studies employing highly-accurate digital elevation models will perform simple analytical models as well as high resolution three-dimensional models to simulate changing coastlines under a variety of sea-level, tidal forcing, and anthropogenic change scenarios (historical and future) to better understand the tidal dynamics in Hong Kong, and to try to separate the relative importance of local and regional effects.

5. Conclusions

This study has presented new information about the tidal variability in Hong Kong, based on observations of a set of closely-located tide gauges in Hong Kong. The TACs, D_1/D_2 relations, δ-HATs, and the anomalous events in tidal amplitudes seen at the Quarry Bay and Tai Po Kau gauges show an amplified tidal response to MSL fluctuations in these harbor regions as opposed to more open-water locations, where individual TAC were sometimes significant, but not as much for the δ-HATs. The reason for the observed behavior may be due to changing friction or resonance induced by coastal engineering projects that are only significant at highly local (i.e., individual harbor) scales. Alternatively, the observed behavior could be related to regional SCS changes due to climate change (such as increased upper-ocean warming and/or regional stratification and internal tide generation) may also be a factor. It is difficult to separate the local engineering changes from regional climatic changes without closer investigations. However, even without exact knowledge of the relevant mechanisms, these anomalies do suggest that a pronounced change in tidal properties occurred around the year 2000 in Hong Kong, with the effect being most pronounced at gauges in semi-enclosed harbors. Overall, the tidal variability in Hong Kong documented here may have significant impacts on the future of extreme sea level in the region, especially if the strong positive reinforcements hold or increase in coming decades. Short-term inundation events, such as nuisance flooding, may be amplified under scenarios of higher sea-levels that lead to corresponding changes in the tides, which may amplify small changes in water levels and/or reductions in friction due to harbor improvements. The δ-HATs and D_1/D_2 TACs results illustrate that tidal variability can be positively reinforced at some locations, which may further agitate coastal flooding under MSL future rise. Since tides and storm surge are both long-wave processes, the locations of strong tidal response may also experience an exaggerated storm surge in the near future.

Code availability All code employed in this study was developed using MATLAB, version R2011B. All code and methods can be provided upon request.

Data Availability The data used in this study from the Hong Kong Observatory (HKO; www.hko.gov.hk) and the Hong Kong Marine Department (HKMD; www.mardep.gov.hk/en/home.html) was provided upon request, discussion of intentions of use, and permission from the appropriate agency supervisors. Data used from the University of Hawaii Sea Level Center (UHSLC; www.uhslc.soest.hawaii.edu) is publicly available.

Author Contributions ATD did all analyses, figures, tables, the majority of writing, and complied the manuscript. JP provided editing, insight, guidance, and direction to this study. HL provided critical insight and helpful input.

Competing Interests The authors declare they have no competing interest.

Acknowledgements This work is supported by The National Basic Research Program of China (2015CB954103), the National Natural Science Foundation of China (project 41376035), the General Research Fund of Hong Kong Research Grants Council (RGC) (CUHK 14303818, 402912, and 403113), the Hong Kong Innovation and Technology Fund under the grants (ITS/259/12 and ITS/321/13), and the direct grants of the Chinese University of Hong Kong.

FIGURE CAPTIONS:

Figure 1 Tide gauge locations in Hong Kong used in this study. Green markers indicate active gauges provided by the Hong Kong Observatory (HKO), light blue markers indicate gauges provided by the Hong Kong Marine Department (HKMD), and red markers indicate historical gauges (once maintained by HKO) that are no longer operational.

Figure 2 Location of Hong Kong in the South China Sea (SCS), given by the red box, with some major oceanographic features labelled. Depth is given by the color bar, in units of meters.

Figure 3 Tidal anomaly correlations (TACs) of detrended M_2 amplitude to detrended MSL in Hong Kong, with the marker size showing the relative magnitude according to the legend, in units of mm m^{-1}. Black marks indicate insignificant TACs.

Figure 4 Tidal anomaly correlations (TACs) of detrended S_2 amplitude to detrended MSL in Hong Kong, with the marker size showing the relative magnitude according to the legend, in units of mm m^{-1}. Black marks indicate insignificant TACs.

Figure 5 Tidal anomaly correlations (TACs) of detrended K_1 amplitude to detrended MSL in Hong Kong, with the marker size showing the relative magnitude according to the legend, in units of mm m^{-1}. Black marks indicate insignificant TACs.

Figure 6 Tidal anomaly correlations (TACs) of detrended O_1 amplitude to detrended MSL in Hong Kong, with the marker size showing the relative magnitude according to the legend, in units of mm m^{-1}. Black marks indicate insignificant TACs.

Figure 7 The change in the highest astronomical tide (δ-HAT), given by the detrended sum of the $M_2 + S_2 + K_1 + O_1$ amplitudes to detrended MSL in Hong Kong, with the marker size showing the relative magnitude according to the legend, in units of mm m^{-1}. Black marks indicate insignificant TACs.

Figure 8 The OT TACs; the relations of detrended diurnal tidal amplitude sum (D_1; $K_1 + O_1$) to detrended semidiurnal tidal amplitude sum (D_2; $M_2 + S_2$) in Hong Kong, with the marker size showing the relative magnitude according to the legend, in dimensionless units. Black marks indicate insignificant TACs.

Figure 9 Time series of water level spectrum components at the Quarry Bay (QB; blue) and Tai Po Kau (TPK; red) tide gauges in Hong Kong, showing the D_1 band (a), the D_2 band (b), the OT band (c) and mean sea-level (MSL) (d). Components are plotted as a function of normalized amplitudes to show relative variability, with mean values given in the legend.

FIGURES:

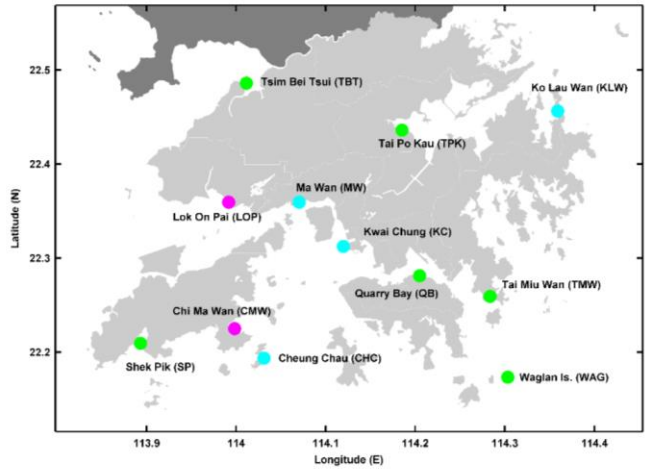

Figure 1 Tide gauge locations in Hong Kong used in this study. Green markers indicate active gauges provided by the Hong Kong Observatory (HKO), light blue markers indicate gauges provided by the Hong Kong Marine Department (HKMD), and red markers indicate historical gauges (once maintained by HKO) that are no longer operational.

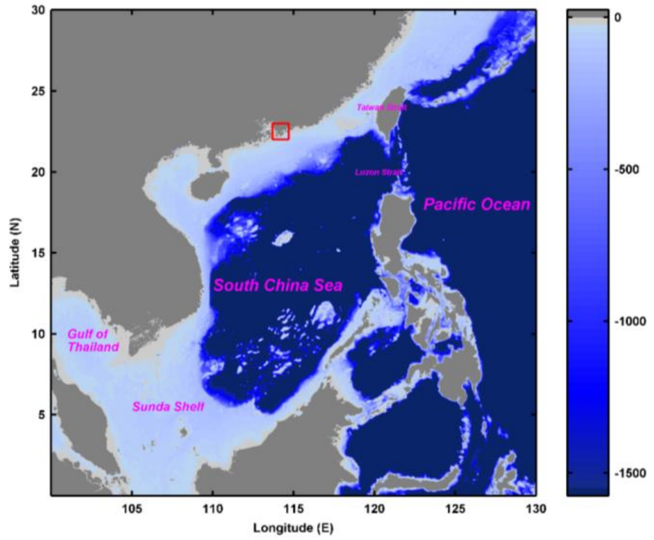

Figure 2 Location of Hong Kong in the South China Sea (SCS), given by the red box, with some major oceanographic features labelled. Depth is given by the color bar, in units of meters.

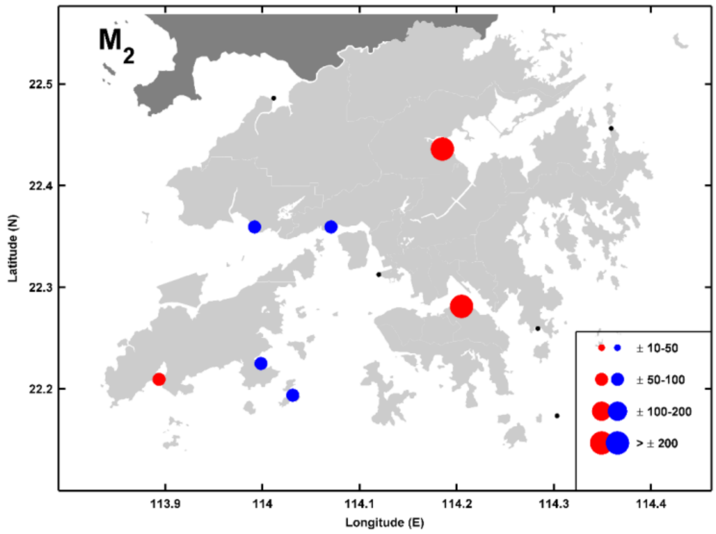

Figure 3 Tidal anomaly correlations (TACs) of detrended M_2 amplitude to detrended MSL in Hong Kong, with the marker size showing the relative magnitude according to the legend, in units of mm m^{-1}. Black marks indicate insignificant TACs.

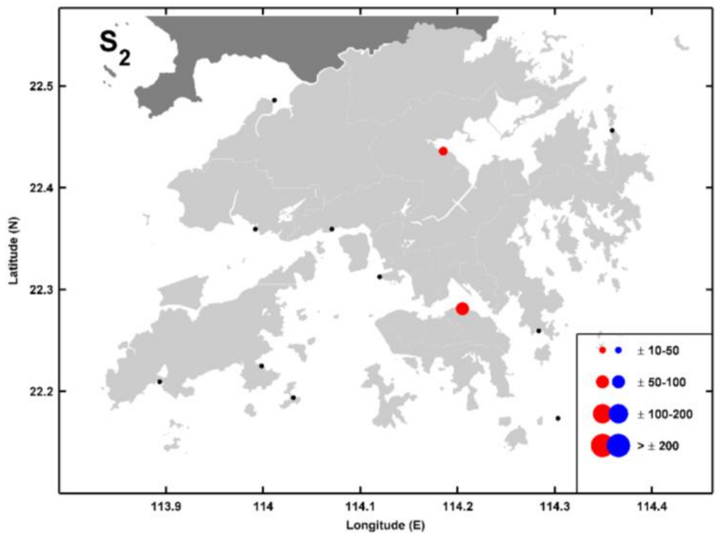

Figure 4 Tidal anomaly correlations (TACs) of detrended S_2 amplitude to detrended MSL in Hong Kong, with the marker size showing the relative magnitude according to the legend, in units of mm m^{-1}. Black marks indicate insignificant TACs.

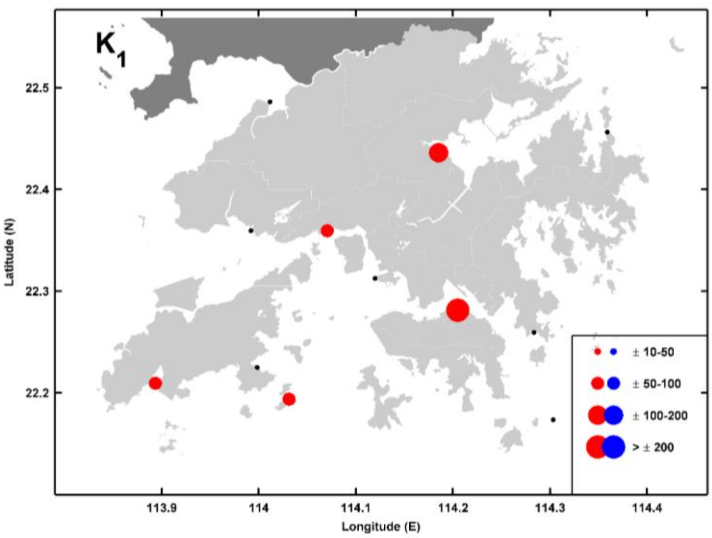

Figure 5 Tidal anomaly correlations (TACs) of detrended K_1 amplitude to detrended MSL in Hong Kong, with the marker size showing the relative magnitude according to the legend, in units of mm m^{-1}. Black marks indicate insignificant TACs.

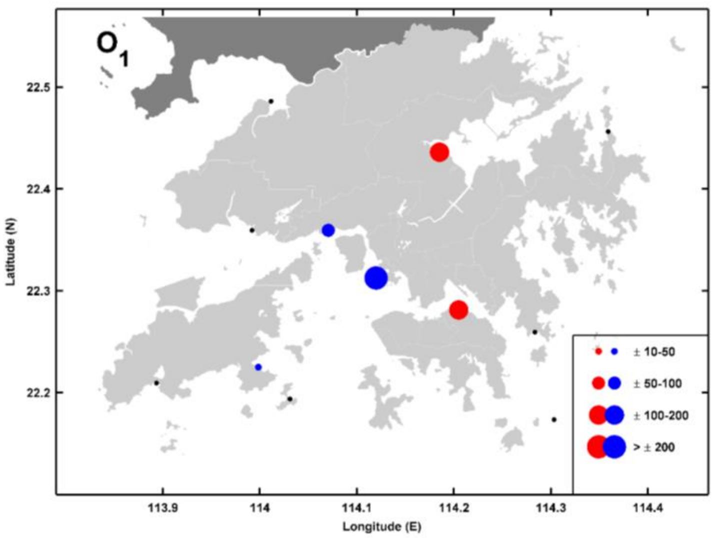

Figure 6 Tidal anomaly correlations (TACs) of detrended O_1 amplitude to detrended MSL in Hong Kong, with the marker size showing the relative magnitude according to the legend, in units of mm m^{-1}. Black marks indicate insignificant TACs.

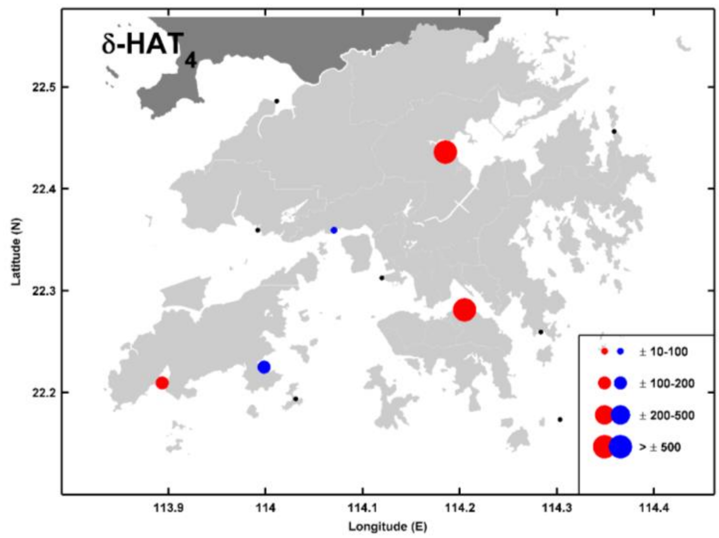

Figure 7 The change in the highest astronomical tide (δ-HAT), given by the detrended sum of the $M_2 + S_2 + K_1 + O_1$ amplitudes to detrended MSL in Hong Kong, with the marker size showing the relative magnitude according to the legend, in units of mm m^{-1}. Black marks indicate insignificant TACs.

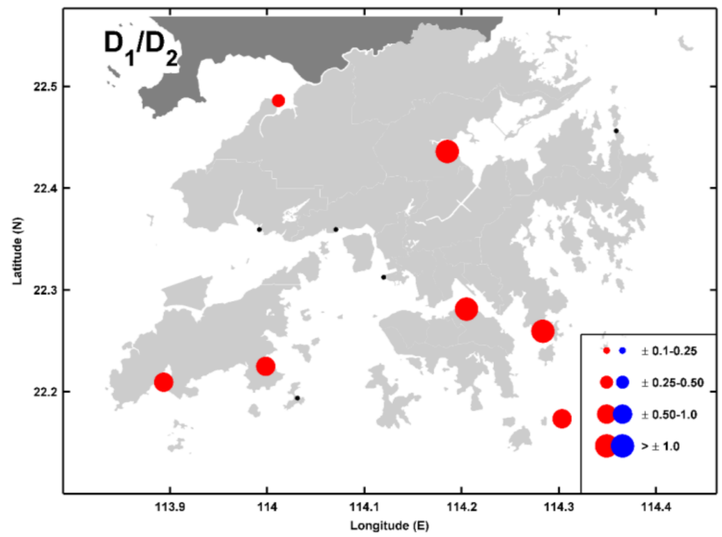

Figure 8 The OT TACs; the relations of detrended diurnal tidal amplitude sum (D_1; $K_1 + O_1$) to detrended semidiurnal tidal amplitude sum (D_2; $M_2 + S_2$) in Hong Kong, with the marker size showing the relative magnitude according to the legend, in dimensionless units. Black marks indicate insignificant TACs.

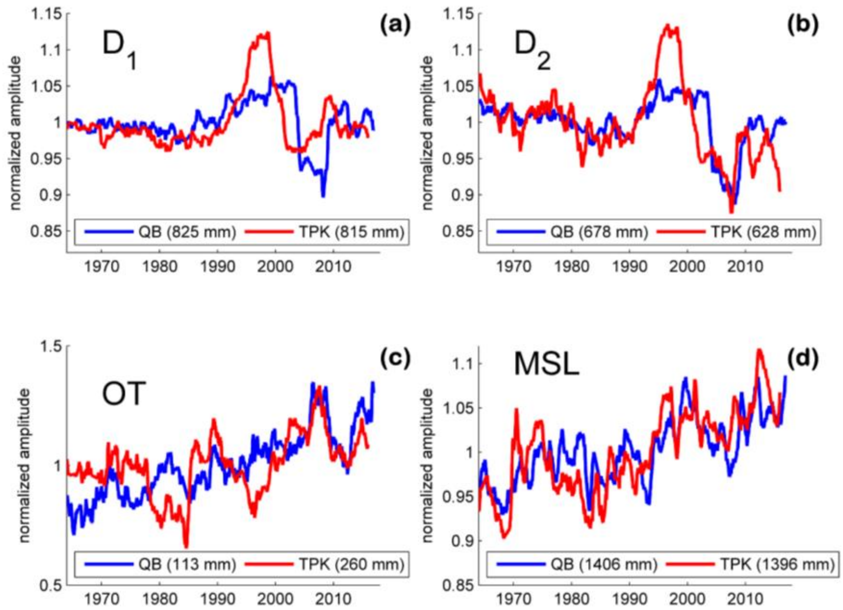

Figure 9 Time series of water level spectrum components at the Quarry Bay (QB; blue) and Tai Po Kau (TPK; red) tide gauges in Hong Kong, showing the D_1 band (a), the D_2 band (b), the OT band (c) and mean sea-level (MSL) (d). Components are plotted as a function of normalized amplitudes to show relative variability, with mean values given in the legend.

REFERENCES:

Alford, M. H.: Observations of parametric subharmonic instability of the diurnal internal tide in the South China Sea. *Geophysical Research Letters*, 35, L15602, 2008. doi:10.1029/2008GL034720

Amin, M.: On perturbations of harmonic constants in the Thames Estuary. Geophysical Journal of the Royal Astronomical Society. *73*(3): 587-603. doi:10.1111/j.1365-246X.1983.tb03334.x, 1983.

Arbic, B.K., Karsten, R.H., Garrett, C.: On tidal resonance in the global ocean and the back-effect of coastal tides upon open-ocean tides. *Atmosphere-Ocean 47*(4), 239–266. doi:10.3137/OC311.2009, 2009.

Arns, A., Dangendorf, S., Jensen, J., Bender, J., Talke, S.A., & Pattiaratchi, C.: Sea-level rise induced amplification of coastal protection design heights. *Nature: Scientific Reports*,*7*, 40171. doi:10.1038/srep40171, 2017.

Bowen, A. J., & Gray, D. A.: The tidal regime of the River Thames; long-term trends and their possible causes. *Phil. Trans. R. Soc. Lond. A*, *272*(1221), 187-199. doi:10.1098/rsta.1972.0045, 1972.

Buchanan, M. K., Oppenheimer, M., & Kopp, R. E.: Amplification of flood frequencies with local sea level rise and emerging flood regimes. *Environmental Research Letters*, *12*(6), 064009. doi:10.1088/1748-9326/aa6cb3, 2017.

Cartwright, D.E., & Tayler, R.J.: New computations of the tide-generating potential. *Geophys. Journal of the Royal Astronomical Society*, *23*, 45-74. doi: 10.1111/j.1365-246X.1971.tb01803.x, 1971.

Cartwright, D.E.: Secular changes in the oceanic tides at Brest, 1711–1936. *Geophysical Journal International*, 30(4), 433-449. doi:10.1.1.867.2468, 1972.

Chernetsky, A. S., Schuttelaars, H. M., & Talke, S. A.: The effect of tidal asymmetry and temporal settling lag on sediment trapping in tidal estuaries. *Ocean Dynamics*, *60*(5), 1219-1241.. doi: 10.1007/s10236-010-0329-8, 2010.

Cherqui, F., Belmeziti, A., Granger, D., Sourdril, A., & Le Gauffre, P.: Assessing urban potential flooding risk and identifying effective risk-reduction measures. *Science of the Total Environment*, *514*, 418-425, 2015.

Chinn, B. S., Girton, J. B., & Alford, M. H.: Observations of internal waves and parametric subharmonic instability in the Philippines archipelago. *Journal of Geophysical Research: Oceans*, *117*(C5). doi:10.1029/2011JC007392, 2012.

Church, J. A., & White, N. J.: A 20th century acceleration in global sea-level rise. *Geophysical research letters*, *33*(1). doi:10.1029/2005GL024826, 2006.

Church, J. A., & White, N. J.: Sea-level rise from the late 19th to the early 21st century. *Surveys in geophysics*, *32*(4-5), 585-602. doi 10.1007/s10712-011-9119-1, 2011.

Colosi, J. A., & Munk, W.: Tales of the venerable Honolulu tide gauge. *Journal of physical oceanography*, *36*(6), 967-996. doi:10.1175/JPO2876.1, 2006.

Craik, A.D.D.: Wave Interactions and Fluid Flows. Cambridge Univ. Press, Cambridge, U. K, ISBN: 978-0521368292, 1985.

Devlin, A. T., Jay, D. A., Talke, S. A., & Zaron, E.: Can tidal perturbations associated with sea level variations in the western Pacific Ocean be used to understand future effects of tidal evolution? *Ocean Dynamics*, *64*(8), 1093-1120. doi:10.1007/s10236-014-0741-6, 2014.

Devlin, A. T., Jay, D. A., Zaron, E. D., Talke, S. A., Pan, J., & Lin, H.: Tidal variability related to sea level variability in the Pacific Ocean. *Journal of Geophysical Research: Oceans*, *122*(11), 8445-8463. doi:10.1002/2017JC013165, 2017.

Devlin, A. T., Jay, D. A., Talke, S. A., Zaron, E. D., Pan, J., & Lin, H.: Coupling of sea level and tidal range changes, with implications for future water levels. *Scientific Reports*, *7*(1), 17021. doi:10.1038/s41598-017-17056-z, 2017.

Devlin, A. T., Zaron, E. D., Jay, D. A., Talke, S. A., & Pan, J.: Seasonality of Tides in Southeast Asian Waters. *Journal of Physical Oceanography*. doi: 10.1175/JPO-D-17-0119.1, 2018.

Devlin, A. T., Pan, J., & Lin, H.: Extended spectral analysis of tidal variability in the North Atlantic Ocean. Journal of Geophysical Research: Oceans, 124(1), 506-526, 2019.

Domingues, C. M., Church, J. A., White, N. J., Gleckler, P. J., Wijffels, S. E., Barker, P. M., & Dunn, J. R.: Improved estimates of upper-ocean warming and multi-decadal sea-level rise. *Nature*, *453*(7198), 1090. doi:10.1038/nature07080, 2008.

Haigh, I. D., Wijeratne, E. M. S., MacPherson, L. R., Pattiaratchi, C. B., Mason, M. S., Crompton, R. P., & George, S.: Estimating present day extreme water level exceedance probabilities around the coastline of Australia: tides, extra-tropical storm surges and mean sea level. *Climate Dynamics*, *42*(1-2), 121-138. doi: 10.1007/s00382-012-1652-1, 2014.

Familkhalili, R., & Talke, S. A.: The effect of channel deepening on tides and storm surge: A case study of Wilmington, NC. *Geophysical Research Letters*, *43*(17), 9138-9147. doi:10.1002/2016GL069494, 2016.

Fang, G., Kwok, Y. K., Yu, K., & Zhu, Y.: Numerical simulation of principal tidal constituents in the South China Sea, Gulf of Tonkin and Gulf of Thailand. *Continental Shelf Research*, *19*(7), 845-869. doi: 10.1016/S0278-4343(99)00002-3, 1999.

Feng, X., Tsimplis, M. N., & Woodworth, P. L.: Nodal variations and long-term changes in the main tides on the coasts of China. *Journal of Geophysical Research: Oceans*, *120*(2), 1215-1232. doi:10.1002/2014JC010312, 2015.

Ip, S.F. and Wai, H.G.: *An application of harmonic method to tidal analysis and prediction in Hong Kong*. Royal Observatory, 1990.

Jan, S., Chern, C. S., Wang, J., & Chao, S. Y.: Generation of diurnal K_1 internal tide in the Luzon Strait and its influence on surface tide in the South China Sea. *Journal of Geophysical Research: Oceans*, *112*(C6). doi:10.1029/2006JC004003, 2007.

Jan, S., Lien, R. C., & Ting, C. H.: Numerical study of baroclinic tides in Luzon Strait. *Journal of Oceanography*, *64*(5), 789. doi:10.1007/s10872-008-0066-5, 2008.

Jay, D. A. (2009). Evolution of tidal amplitudes in the eastern Pacific Ocean. *Geophysical Research Letters*, *36*(4). doi: 10.1029/2008GL036185

Leffler, K. E., & Jay, D. A.: Enhancing tidal harmonic analysis: Robust (hybrid L1/L2) solutions. *Continental Shelf Research*, *29*(1), 78-88. doi: 10.1016/j.csr.2008.04.011, 2009.

Li, K. W., & Mok, H. Y.: Long term trends of the regional sea level changes in Hong Kong and the adjacent waters. In *Asian And Pacific Coasts 2011* (pp. 349-359). doi:10.1142/9789814366489_0040, 2012.

Lien, R. C., Tang, T. Y., Chang, M. H., & d'Asaro, E. A.: Energy of nonlinear internal waves in the South China Sea. *Geophysical Research Letters*, *32*(5). doi:10.1029/2004GL022012, 2005.

MacKinnon, J. A., & Winters, K. B.: Subtropical catastrophe: Significant loss of low-mode tidal energy at 28.9°. *Geophysical Research Letters*, *32*(15). doi:10.1029/2005GL023376, 2005.

Mawdsley, R. J., Haigh, I. D., & Wells, N. C.: Global changes in mean tidal high water, low water and range. *Journal of Coastal Research*, *70*(sp1), 343-348. doi:10.2112/SI70-058.1, 2014.

McComas, C. H., & Bretherton, F. P.: Resonant interaction of oceanic internal waves. *Journal of Geophysical Research*, *82*(9), 1397-1412. doi:10.1029/JC082i009p01397, 1977.

Moftakhari, H. R., AghaKouchak, A., Sanders, B. F., Feldman, D. L., Sweet, W., Matthew, R. A., & Luke, A.: Increased nuisance flooding along the coasts of the United States due to sea level rise: Past and future. *Geophysical Research Letters*, *42*(22), 9846-9852. doi:10.1002/2015GL066072, 2015.

Moftakhari, H. R., AghaKouchak, A., Sanders, B. F., & Matthew, R. A.: Cumulative hazard: The case of nuisance flooding. *Earth's Future*, *5*(2), 214-223. doi:10.1002/2016EF000494, 2017.

Müller, M., Arbic, B. K., & Mitrovica, J. X.: Secular trends in ocean tides: Observations and model results. *Journal of Geophysical Research: Oceans*, *116*(C5) doi: 10.1029/2010JC006387, 2011.

Müller, M., Cherniawsky, J. Y., Foreman, M. G. G., & Storch, J. S.: Global M_2 internal tide and its seasonal variability from high resolution ocean circulation and tide modeling. *Geophysical Research Letters*, *39*(19). doi:10.1029/2012GL053320, 2012.

Müller, M.: The influence of changing stratification conditions on barotropic tidal transport and its implications for seasonal and secular changes of tides. *Continental Shelf Research*, *47*, 107-118. doi: 10.1016/j.csr.2012.07.003, 2012.

Pan, J., Gu, Y. and Wang, D.: Observations and numerical modeling of the Pearl River plume in summer season, *Journal of Geophysical Research*, 119, doi:10.1002/2013JC009042, 2014.

Pawlowicz, R., Beardsley, B., & Lentz, S.: Classical tidal harmonic analysis including error estimates in MATLAB using T_TIDE. *Computers & Geosciences*, *28*(8), 929-937. doi:10.1016/S0098-3004(02)00013-4, 2002.

Rasheed, A. S., & Chua, V. P.: Secular trends in tidal parameters along the coast of Japan. *Atmosphere-Ocean*, *52*(2), 155-168. doi:10.1080/07055900.2014.886031, 2014.

Ray, R. D.: Secular changes of the M_2 tide in the Gulf of Maine. *Continental shelf research*, *26*(3), 422-427. doi: 10.1016/j.csr.2005.12.005, 2006.

Ray, R. D., & Foster, G.: Future nuisance flooding at Boston caused by astronomical tides alone. *Earth's Future*, *4*(12), 578-587. doi:10.1002/2016EF000423, 2016.

Ross, A. C., Najjar, R. G., Li, M., Lee, S. B., Zhang, F., & Liu, W.: Fingerprints of Sea Level Rise on Changing Tides in the Chesapeake and Delaware Bays. *Journal of Geophysical Research: Oceans*, *122*(10), 8102-8125. doi:10.1002/2017JC012887, 2017.

Sweet, W. V., & Park, J.: From the extreme to the mean: Acceleration and tipping points of coastal inundation from sea level rise. *Earth's Future*, 2(12), 579-600, 2014.

Vellinga, N. E., Hoitink, A. J. F., van der Vegt, M., Zhang, W., & Hoekstra, P.: Human impacts on tides overwhelm the effect of sea level rise on extreme water levels in the Rhine–Meuse delta. *Coastal Engineering*, *90*, 40-50. doi: 10.1016/j.coastaleng.2014.04.005, 2014.

Woodworth, P. L.: A survey of recent changes in the main components of the ocean tide. *Continental Shelf Research*, *30*(15), 1680-1691. doi: 10.1016/j.csr.2010.07.002, 2010.

Xie, X. H., Chen, G. Y., Shang, X. D., & Fang, W. D.: Evolution of the semidiurnal (M2) internal tide on the continental slope of the northern South China Sea. *Geophysical Research Letters*, *35*(13). doi:10.1029/2008GL034179, 2008.

Xie, X. H., Shang, X. D., van Haren, H., Chen, G. Y., & Zhang, Y. Z.: Observations of parametric subharmonic instability-induced near-inertial waves equatorward of the critical diurnal latitude. *Geophysical Research Letters*, *38*(5). doi:10.1029/2010GL046521, 2011.

Xie, X., Shang, X., Haren, H., & Chen, G.: Observations of enhanced nonlinear instability in the surface reflection of internal tides. *Geophysical Research Letters*, *40*(8), 1580-1586. doi:10.1002/grl.50322, 2013.

Zaron, E. D., & Jay, D. A.: An analysis of secular change in tides at open-ocean sites in the Pacific. *Journal of Physical Oceanography*, *44*(7), 1704-1726. doi:10.1175/JPO-D-13-0266.1, 2014.

Zhang, H., Wang, T., Liu, M., Jia, M., Lin, H., Chu, L. M., & Devlin, A. T.: Potential of Combining Optical and Dual Polarimetric SAR Data for Improving Mangrove Species

Discrimination Using Rotation Forest. *Remote Sensing*, *10*(3), 467. doi: 10.3390/rs10030467, 2018.

Formatted: English (United States)

TABLES:

Table 1 Metadata for all tide gauge locations, giving latitude/longitude, and start year/end year of the full record, as well as of data analyzed in this study.

Station	*Latitude*	*Longitude*	*Start Year*	*End Year*	*Number of years used*
Quarry Bay (QB)	22.27° N	114.21° E	1954	2016	30 (1986-2016)
Tai Po Kau (TPK)	22.42° N	114.19° E	1963	2016	30 (1986-2016)
Tsim Bei Tusi (TBT)	22.48° N	114.02° E	1974	2016	30 (1986-2016)
Chi Ma Wan (CMW)	22.22° N	114.00° E	1963	1997	36 (1963-1997)
Cheung Chau (CHC)	22.19° N	114.03° E	2004	2016	12 (2004-2016)
Lok On Pai (LOP)	22.35° N	114.00° E	1981	1999	18 (1981-1999)
Ma Wan (MW)	22.35° N	114.06° E	2004	2016	12 (2004-2016)
Tai Miu Wan (TMW)	22.26° N	114.29° E	1996	2016	20 (1996-2016)
Shek Pik (SP)	22.21° N	113.89° E	1999	2016	17 (1999-2016)
Waglan Island (WAG)	22.17° N	114.30° E	1995	2016	21 (1995-2016)
Ko Lau Wan (KLW)	22.45° N	114.34° E	2004	2016	12 (2004-2016)
Kwai Chung (KC)	22.31° N	114.12° E	2004	2016	12 (2004-2016)

Table 2 Amplitude TACs for M_2, S_2, K_1, and O_1. All values given are in units of millimeter change in tidal amplitude for a 1-meter fluctuation in sea-level (mm m^{-1}). Statistically significant positive values are given in bold italic text.

Station	**M_2 TAC**	**S_2 TAC**	**K_1 TAC**	**O_1 TAC**
Quarry Bay (QB)	***+218 ± 37***	***+85 ± 16***	***+220 ± 15***	***+146 ± 11***
Tai Po Kau (TPK)	***+267 ± 42***	***+98 ± 17***	***+190 ± 68***	***+100 ± 25***
Tsim Bei Tusi (TBT)	+7 ± 80	-10 ± 15	+32 ± 22	+24 ± 22
Chi Ma Wan (CMW)	***-58 ± 11***	-7 ± 5	-18 ± 8	***-37 ± 10***
Cheung Chau (CHC)	***-63 ± 20***	-22 ± 35	***+69 ± 48***	+50 ± 92
Lok On Pai (LOP)	***-81 ± 24***	-18 ± 8	+8 ± 32	-24 ± 12
Ma Wan (MW)	***-68 ± 4***	+1 ± 25	***+52 ± 4***	***-62 ± 21***
Tai Miu Wan (TMW)	+22 ± 59	-1 ± 9	+10 ± 22	+3 ± 8
Shek Pik (SP)	***+62 ± 29***	+11 ± 18	***+70 ± 4***	+28 ± 17
Waglan Island (WAG)	+1 ± 21	+3 ± 6	+9 ± 7	-9 ± 8
Ko Lau Wan (KLW)	-46 ± 39	-11 ± 17	+29 ± 65	+60 ± 57
Kwai Chung (KC)	-90 ± 46	-10 ± 29	-91 ± 226	***-202 ± 161***

Table 3 The δ-HAT and D_1/D_2 TACs. The δ-HAT values given are in units of millimeter change in tidal amplitude for a 1-meter fluctuation in sea-level (mm m^{-1}). D_1/D_2 TACs are in unitless ratios (i.e., mm mm^{-1}) Statistically significant values are given in bold italic text.

Station	**δ-HAT**	**D_1/D_2**
Quarry Bay (QB)	***+665 ± 82***	***+1.08 ± 0.05***
Tai Po Kau (TPK)	***+612 ± 210***	***+1.01 ± 0.04***
Tsim Bei Tusi (TBT)	+56 ± 117	***+0.37 ± 0.02***
Chi Ma Wan (CMW)	***-119 ± 19***	***+0.74 ± 0.19***
Cheung Chau (CHC)	-12 ± 42	+0.81 ± 1.03
Lok On Pai (LOP)	-114 ± 45	***+0.26 ± 0.05***
Ma Wan (MW)	***-91 ± 73***	+0.57 ± 1.02
Tai Miu Wan (TMW)	+42 ± 100	***+1.04 ± 0.20***
Shek Pik (SP)	***+138 ± 37***	***+0.89 ± 0.06***
Waglan Island (WAG)	+3 ± 31	***+1.11 ± 0.17***
Ko Lau Wan (KLW)	-66 ± 47	***+1.31 ± 0.62***

Tidal variability in the Hong Kong region

Adam T. Devlin

Institute of Space and Earth Information Science, The Chinese University of Hong Kong, Shatin, Hong Kong SAR, China

Jiayi Pan*

Institute of Space and Earth Information Science, The Chinese University of Hong Kong, Shatin, Hong Kong SAR, China

College of Marine Science, Nanjing University of Information Science and Technology, Nanjing, Jiangsu, China

Shenzhen Research Institute, The Chinese University of Hong Kong, Shenzhen, Guangdong, China

Hui Lin

Institute of Space and Earth Information Science, The Chinese University of Hong Kong, Shatin, Hong Kong SAR, China

* Corresponding author

Abstract

Mean sea level (MSL) is rising worldwide, and correlated changes in ocean tides are also occurring; their combination may influence future total sea levels (TSL), possibly increasing coastal inundation and nuisance flooding events in sensitive regions. Analyses of a set of tide gauges in Hong Kong and in the South China Sea (SCS) reveal complex tidal behavior. Most prominent in the results are strong correlations of MSL variability to tidal variability which may further increase local flood levels under future MSL rise. We also highlight inter-tidal correlations of diurnal (D_1) tides to semidiurnal (D_2) tides, positively reinforced through the northern SCS, and the correlations of overtide (OT) fluctuations to D_1 and D_2, negatively reinforced (i.e., anti-correlated) across the same region, thought to be related to the baroclinic energetics in the Luzon Strait and the Taiwan Strait. The baroclinic signals may be enhanced at the northern shelf of the SCS and can generate PSI interactions that may amplify minor tides such as M_3. Additionally, there are anomalous tidal events observed in some enclosed harbor regions of Hong Kong, corresponding to times of rapidly changing MSL as well as rapid coastal development projects. Results support the hypothesis that the observed variability is due to multiple spatial processes, best described as an amplification of the local (Hong Kong) tidal response to the prevailing regional (SCS) tidal patterns, enhanced by local harbor changes. A close analysis of the full-spectrum tidal response suggests that a change in the resonant and frictional response may have occurred.

1. Introduction

Ocean tides have long been considered to be a stationary process, as they are driven by the gravitational forcing of the Sun and Moon whose motions are complex but highly predictable (Cartwright and Tayler, 1971). Yet, long-term changes in the tides have been observed recently on regional (Ray, 2006; Jay et al., 2009; Zaron and Jay, 2014; Rasheed and Chua, 2014; Feng et al., 2015; Ross et al., 2017) and worldwide spatial scales (Woodworth, 2010; Müller, et al. 2011; Haigh et al., 2014; Mawdsley et al., 2015), concurrent with long-term global mean sea level (MSL) rise (Church and White, 2006; 2011). Since gravitational changes are not the reason, the tidal changes are likely related to terrestrial factors such as: changes in water depth which can alter friction (Arbic et al, 2009), coastal morphology and resonance changes of harbor regions (Cartwright, 1972; Bowen and Gray, 1972; Amin, 1983; Vellinga et al., 2014; Jay et al., 2011; Chernetsky et al., 2010, Familkhalili & Talke, 2016), or stratification changes induced by increased upper-ocean warming (Domingues et al., 2008; Colosi and Munk, 2006; Müller, 2012; Müller et al., 2012), all of which are also related to sea-level rise. Tides can also exhibit short-term variability correlated to short-term fluctuations in MSL. These variabilities may influence extreme water level events, such as storm surge or nuisance flooding (Sweet and Park, 2014; Cherqui et al., 2015; Moftakhari et al., 2015; 2017; Ray and Foster, 2016). Such short-term extreme events are obscured when only considering long-term linear trends. Any significant additional positive correlation between tides and sea-level fluctuations may amplify this effect and implies that flood risk based only on the superposition of present day tides and surge onto a higher baseline sea-level will be inaccurate in many situations. The accurate determination of the nature and impact of sea-level rise and associated tidal change necessitates a regionally- and locally-focused strategy, therefore, analysis of the correlations between tides and sea level can indicate locations where tidal evolution should be considered a substantial modification to sea-level rise. Moreover, since storm surge is a long wave, factors affecting tides can also alter storm surge (Familkhalil and Talke, 2016; Arns et al., 2017), so an improved knowledge of tides can also improve storm response planning and may be instructive in guiding future coastal development.

Recent works have surveyed tidal anomaly correlations (TACs) at multiple locations in the Pacific, examining the sensitivity of tides to sea-level fluctuations (Devlin et al., 2014; Devlin, 2016; Devlin et al., 2017a), finding that over 90% of tide gauges analyzed exhibited some measure of correlation in at least one tidal component. In a related work (Devlin et al., 2017b), the combined TACs of the four largest tidal components was calculated as a proxy for the changes in the highest astronomical tide (δ-HAT), with 35% of gauges surveyed exhibiting a sensitivity of δ-HATs to sea-level fluctuations of at least ±5% in addition to sea-level change. The greatest δ-HAT response was seen in Hong Kong (+65%), and additional analyses revealed that TSL exceedance levels have nearly doubled (+150 mm) that of MSL exceedance alone (+78 mm) over the past 50 years, demonstrating that the non-stationarity of tides can be a significant contributor to total water levels in this region, and this behavior warrants closer examination.

1.1 Sea-level and tides in Hong Kong and the South China Sea

Hong Kong and the Pearl River Delta (PRD) region contains many densely-populated urban metropolises with extensive coastal infrastructure, and substantial recent land reclamation projects. These coastal morphology changes along with sea-level rise may change the local resonant and frictional response of the local tides to the regional tidal variability and may contribute to TSL changes and nuisance flooding. Sea-level rise in the region has exhibited a variable rate in the region over the past 50 years (Li and Mok, 2012), but a common feature of all sea level records in the SCS is a steep increase in the late 1990s with a subsequent decrease in the early 2000s, then followed by a sustained increase to the present day. In addition to the variable MSL behavior, there are also anomalous tidal events observed at gauges in semi-enclosed harbor regions during the late 1990s and early 2000s (shown and discussed below), corresponding to times of both rapidly changing sea level and aggressive land reclamation.

Understanding the tidal behavior in Hong Kong requires a thorough examination of the tidal dynamics in the South China Sea. Both diurnal (D_1) and semidiurnal (D_2) tides enter the SCS from the Pacific through the Luzon Strait. The D_2 constituents are damped by a factor of two as they enter the SCS, and the D_1 constituents are amplified by a similar factor (Zu et al., 2008; Fang et al., 1999; Jan et al., 2007). The semidiurnal wave bifurcates, partially travelling northwest towards the Taiwan Strait, and partially travelling southwest towards the Sunda Shelf, though the diurnal wave only propagates southwest. The part of the semidiurnal wave that travels towards the Taiwan Strait meets the large incoming semidiurnal energy from the East China Sea (ECS). The semidiurnal tides have very large amplitudes (~ 2m) here and exhibit a D_2 resonance on the western side of the Strait via a partial quarter-wave resonance (Jan et al., 2004). In addition, a large amount of D_2 internal energy is generated, though little to no D_1 baroclinic energy is observed.

The Luzon region is one of the most active regions of baroclinic generation in the world ocean (Wang, 2012). Approximately one third of the K_1 surface tide energy (~ 12 GW) is converted to baroclinic energy (Jan et al. 2007), and about one quarter of the M_2 surface tide is converted to the baroclinic tide (Niwa and Hibiya, 2004). The surface tide expression in the SCS is dependent on the baroclinic conversion, which is in turn highly sensitive to the geometric and environmental properties of the Luzon Strait (Jan et al., 2008; Wang, 2012). Internal tides yield a high-mode vertical velocity structure that tends to dissipate tidal energy close to the generation site as well as a low-mode energy that can travel for thousands of kilometers (Liu et al., 2015). Therefore, even at a great distance from the generation site, much of the baroclinic energy may remain coherent. Internal tides can propagate as narrow beams, which may be enhanced upon arrival at the shelf (Lien et al., 2005), and nonlinear interactions are enhanced within the tidal beams, in areas where internal tide beams are reflected (Mercier et al., 2012), or in regions where the tidal beams intersect (Teoh et al., 1997; Korobov and Lamb, 2008).

The D_1 and D_2 internal tides may interact with each other as well as with other frequencies, such as the local inertial frequency, *f*, via parametric subharmonic instability (PSI) interactions (McComas and Bretherton, 1977; MacKinnon and Winters, 2005), a form of resonant triad interactions (Craik, 1985). Previously, such interactions were only thought to occur near the critical latitude (~29° for M_2) where *f* is equal to half the M_2 frequency (see e.g., Alford, 2008). However, for the case where a PSI interaction turns from weakly nonlinear to strongly nonlinear, it can enhance generation at subharmonics different from exactly half the frequency (Korobov and Lamb, 2008). For example, the presence of a resonant triad interaction between M_2 and K_1*O_1 was observed in the Solomon Sea (Devlin et al., 2014). Many PSI-type tidal interactions have been observed in the SCS. Kinetic energy spectra from a current profiler on the northern continental slope near Dongsha Island (~20° N), halfway between the Luzon Strait and Hong Kong) revealed strong peaks at the nonlinear interaction frequencies of fM_1 ($f + M_1$) and M_3 ($M_1 + M_2$), (Xie et al., 2008) as well as other components in the D_3 band (e.g., MO_3). The presence of the PSI interactions was confirmed by bicoherence estimates (Carter and Gregg, 2006), and validates previous suggestions that PSI interactions can occur equatorward of the critical latitudes depending on stratification and circulation conditions (Xie et al, 2011). Other PSI interactions were observed in the southern regions of the SCS (Chinn, 2012; Liu, 2015).

1.2 Outline of this study

It is hypothesized that the observed tidal variability in Hong Kong is due to either: 1) regional changes in the dynamics of the SCS such as MSL rise, circulation patterns, or upper-ocean warming and stratification, 2) local changes in friction and/or resonance related to land reclamation projects, or 3) a combination of coupled mechanisms at multiple spatial and temporal scales. To determine the relevant scales of variability, we perform a spatial and temporal analysis of tidal sensitivity to MSL variations in Hong Kong and the SCS. This manuscript is structured as follows. After the introduction, the data inventory will be described, and a description of the TAC and δ-HAT methods will be given. Following this will be the results, detailing the spatial and temporal patterns of the TAC and δ-HAT determinations. We will then closely examine extreme tidal anomalies in Hong Kong by analyzing the full tidal response, including minor tidal components, and will compare regional correlations of tidal properties in the historical and modern eras. Following the results, a discussion of relevant spatial scales and mechanisms is presented, as well as future proposed works.

2. Methods

2.1 Data sources

A set of 13 tide gauges in the Hong Kong region were provided by the Hong Kong Observatory (HKO) and the Hong Kong Marine Department (HKMD). The longest record is the North Point/Quarry Bay (QB) tide gauge, located in Victoria Harbor. The gauge was established in 1954 and was relocated from North Point to Quarry Bay in 1986, and the datums were adjusted and quality controlled by HKO to provide a continuous record (Ip and Wai, 1990). Five more gauges are provided by HKO: Tsim Bei Tsui (TBT; 1974-present), Tai Po Kau (TPK; 1963-present), Shek Pik (SP; 1999-presnt), Tai Miu Wan (TMW; 1996-present), and Waglan Island (WAG; 1995-present). In addition, four locations are operated by the HKMD (Cheung Chau; CHC, Kwai Chung; KC, Ma Wan; MW, and Ko Lau Wan; KLW); all have been recording from ~2004 to the present day. Next, there are some additional data records originally operated by HKO that are no longer active (Chi Ma Wan (CMW; 1963-1997) and Lok On Pai (LOP; 1981-1999)). Additionally, historical data from China in the Beibu Gulf and the Taiwan Strait are downloaded from the University of Hawaii

Sea Level Center (UHSLC; website): Shanwei (SW), Zhapo (ZP), Beihei (BH), Haikou (HK), Dongfang (DF), and Xiamen (XM). These data records are all continuous from 1976-1997, except for Xiamen which runs from 1954-1997. Rounding out this inventory are six other locations in the SCS acquired from UHSLC; Manila (MN) in the Philippines (1984-2016), Kaohsiung (KS) and Keelung (KL) in Taiwan (1980-2014), Vung Tau (VT), Vietnam (1986-2002; 2007-2014); Sedili (SD), Malaysia (1986-2016), Bintulu (BT), Malaysia (1992-2016), and one location on the outside of the SCS closest to the Luzon Strait (Ishigaki Island; IG, 1968-2013) to provide a comparison to the tides within the SCS. The TACs and δ-HATs at these last seven locations were already reported on in Devlin et al. (2017a; 2017b), here, they are recalculated with updated data to compare the spatial coherence of tidal dynamics in the SCS to Hong Kong. Gauge locations in Hong Kong are shown in Figure 1, with the gauges from HKO indicated by green markers, gauges from HKMD by light blue, and historical (non-operational) gauges by red. SCS gauges are shown in Figure 2; green indicates gauges that are actively updated, red indicates gauges that have not been updated since 1997. Table 1 lists the metadata for all locations, including latitude, longitude, and record length.

2.2 Tidal admittance calculations

Investigations of tidal behavior rely on a tidal admittance method. An admittance is the unitless ratio of an observed tidal constituent to the corresponding tidal constituent in the astronomical tide generating force expressed as a potential, *V*, divided by the acceleration due to gravity, *g*, to yield $Z_{pot}(t) = V/g$, with units of length that can be compared to tidal elevations, $Z_{obs}(t)$, via harmonic analysis. Yearly harmonic analyses are performed on both $Z_{obs}(t)$ and $Z_{pot}(t)$ at each location, using the R_T_TIDE package for MATLAB (Leffler and Jay, 2009), a robust analysis suite based on T_TIDE (Pawlowicz, 2002). Because nodal and other low-frequency astronomical variabilities are present with similar strengths in both the observed tidal record and in $Z_{pot}(t)$, their effects are eliminated in yearly analyzed admittance time series. The tidal potential is determined based on the methods of Cartwright and Tayler (1971). The result from a single harmonic analysis of $Z_{obs}(t)$ or $Z_{pot}(t)$ determines an amplitude, *A*, and phase, *θ*, at the central time of the analysis window for each tidal constituent, with error estimates. A moving analysis window produces time-series of amplitude, $A(t)$, and phase, $\theta(t)$, with the complex amplitude, $\mathbf{Z}(t)$, given by:

$$\mathbf{Z}(t) = A(t)e^{i\theta(t)} \quad (1)$$

The tidal admittance (**A**) and phase lag (**P**) are formed using Eqs. (2) and (3)

$$\mathbf{A}(t) = abs\left|\frac{\mathbf{Z}_{obs}(t)}{\mathbf{Z}_{pot}(t)}\right|, \qquad (2)$$

$$\mathbf{P}(t) = \theta_{obs}(t) - \theta_{pot}(t). \qquad (3)$$

The harmonic analysis procedure also provides an MSL time-series. For each resultant dataset (MSL, **A** and **P**), the mean and trend are removed from the time series to allow direct comparison of their co-variability. The magnitude of the long-term trends is typically much less than the magnitude of the short-term variability, which is now more apparent in the data (Devlin et al., 2017a).

Tidal sensitivity to sea-level fluctuations is quantified using tidal anomaly correlations (TACs), the relationships of detrended tidal variability to detrended MSL variability. We determine the sensitivity of the amplitude and phase of individual constituents (M_2, S_2, K_1, O_1, N_2, K_2, P_1, and Q_1) to sea-level perturbations at the yearly-analyzed scale. We also consider the change in the highest astronomical tide (δ-HAT), estimated in two ways. First, by combining the yearly analyzed time series of the four largest tidal amplitudes (M_2, S_2, K_1, and O_1), approximately 75% of the full tidal height (δ-HAT_4), and secondly by considering the combination of all eight constituents, approximately 95% of the full tidal height (δ-HAT_8). The latter determination provides a better approximation to the full tidal range, though the former provides a more statistically stable value, as the four minor constituents are more prone to noise and spurious fluctuations. The detrended time series of the δ-HATs are compared to detrended MSL variability in an identical manner as the TACs, and both are expressed in units of millimeter change in tidal amplitude per 1-meter fluctuation in sea-level. These units are adopted for convenience, though in practice, the observed fluctuations in MSL are on the order of ~ 0.25 m. The phase TACs are reported in units of degree change per 1-meter fluctuation in sea-level.

The TAC methodology can also be used to examine correlations between different parts of the tidal spectrum. We also consider the sensitivity of combined diurnal (D_1; $K_1 + O_1 + P_1 + Q_1$) tidal perturbations to semidiurnal (D_2; $M_2 + S_2 + N_2 + K_2$) tidal perturbations (D_1/D_2 TACs). Additionally, we calculate the sensitivity of tidal range to frictional changes, by considering the combined variations of the seven largest overtides (OT; M_4, M_6, S_4, MK_3, MO_3, SN_4, and MN_4), to fluctuations in the combined D_1 and D_2 amplitude (OT TACs). The units of the D_1/D_2 and OT TACs are dimensionless (i.e., mm/mm), and statistics are calculated as above. We assume that the interannual variability captured by all TACs and δ-HATs can be extrapolated to longer time scales, subject to the qualification that the changes remain "small-amplitude", i.e., a 0.5 to 1m change in MSL and a change in tidal amplitude of a few 10s of cm.

The definition of the year window used for harmonic analysis may have an influence on the value of the TAC or δ-HAT, e.g. calendar year (Jan-Dec) vs. water year (Oct-Sep). To provide a better estimate of the overall correlations for all data we take a set of determinations of the correlations using twelve distinct year definitions (i.e., one-year windows running from Jan-Dec, Feb-Jan, …, Dec-Jan.). We take the average of the set of significant determinations (i.e., p-values of < 0.05) as the magnitude of the TAC or δ-HAT. For an estimate of the confidence interval of the TAC or δ-HAT, the interquartile range (middle 50% of the set) is used. A step-by-step description of the TAC and δ-HAT methods, including the details of the calculations of the regressions and statistics can be found in the supplementary materials of Devlin et al. (2017b). For the very long record stations (e.g., QB and TPK), we only consider the past 30 years for TAC and δ-HAT determinations, and for other stations, we use the full record, though some locations are less than 30 years, and some are historical.

We also highlight some anomalous tidal events observed around the turn of the century at certain Hong Kong gauges, and we compare and discuss the coherence and evolution of the tidal behavior in Hong Kong and the SCS via correlation analysis. We consider the eight tides in the D_1 and D_2 band, as well as the $2N_2$, M_3 and MO_3 tides (for reasons that will be made clear later), and MSL. All gauges are compared to the Quarry Bay gauge as the "standard", and we consider a demarcation time between "historical" and "modern" as 1997. For the early record, we use the Hong Kong data at CMW, TPK, LOP, and TBT, the historical data from the mainland of China (to represent the historical SCS). For the modern era, we consider all operational data in Hong Kong, as well as Manila, Vung Tau, Sedili, Ishigaki, and the two Taiwan gauges. We use Ishigaki to represent the Pacific in both time periods. For all comparisons, we only use the data that overlaps the QB record. Due to the nature of the time coverage at our set of gauges, only two gauges will allow a direct comparison in both time periods in Hong Kong (TPK and TBT). However, a few other locations in the historical and modern sub-sets are located close enough to each other to allow a near-direct pairing; Lok On Pai/Ma Wan, and Chi Ma Wan/Cheung Chau.

3. Results

The individual TACs for amplitude and phase in Hong Kong and the SCS are discussed first, followed by the δ-HATs, the D_1/D_2 TACs, and the OT TACs. In all figures, significant positive results will be reported by red markers, significant negative results by blue markers, and insignificant values are shown as black markers. The relative size of the markers will indicate the relative magnitude of the TAC or δ-HAT according the legend scale on each plot. All numerical results for the major amplitude TACs (M_2, S_2, K_1, and O_1) are listed in Table 2, and the δ-HATs, D_1/D_2 TACs, and the OT/ (D_1 +D_2) TACs are listed in Table 3. Phase TACs of the major constituents, minor constituent (N_2, K_2, P_1, Q_1) amplitude TACs, and the other OT TACs (i.e., OT/D_1 and OT/D_2) are reported in Table S1, S2 and S3 of the supplementary material. Phase TACs for the minor constituents are insignificant at all locations and are not reported or plotted. Next, we explore the anomalous tidal events seen at Hong Kong gauges in recent years by analyzing the behavior of major and minor tidal components. Finally, we compare correlations between early and later eras to explore the temporal coherency of tidal behavior.

3.1 Tidal anomaly correlations (TACs)

We first show the semidiurnal TACs in Hong Kong (Figure 3 (a) and (c)) and in the SCS (Figure 3 (b) and (d)). In Hong Kong (Fig 3(a)), the strongest positive M_2 TACs are seen at Quarry Bay (+218 ± 37 mm m^{-1}), and at Tai Po Kau (+267 ± 42 mm m^{-1}), with a smaller positive TAC seen at Shek Pik. In the waters west of Victoria Harbor, all gauges except Kwai Chung exhibit moderate negative TACs. In the SCS (Fig 3(b)), very large and positive TACs are seen at the three stations in the Beibu Gulf (Dongfang, Beihei, and Haikou), with values of +190, +460, and +379 mm m^{-1}, respectively. The semidiurnal phase TACs in Hong Kong (shown in the Supplementary materials, Figure S1(a)) show an earlier M_2 tide under higher MSL at QB and TPK (-15 ± 2 and -28 ± 6 deg m^{-1}, respectively), and a later tide west of Victoria Harbor. In the SCS (Fig S1(b)), later tides are observed at Manila, Kaohsiung, and Shanwei, while earlier tides are seen in the Beibu Gulf and at Xiamen. The S_2 results in Hong Kong (Fig 3(c)) reveal that only QB and TPK have significant amplitude TAC values (though smaller than M_2), and the rest of the SCS has a nearly identical spatial distribution as M_2 (Fig 3(d)). The S_2 phase TACs in Hong Kong (Figure S1(c)) again show an earlier tide at QB and TPK under higher MSL, and results in the SCS (Figure S1(d)) are also similar to M_2. The minor semidiurnal amplitude TACs are mainly insignificant in Hong

Kong, though N_2 has a significant positive TAC at TPK of +85 ± 12 mm m^{-1} (Figure S2(a)), and K_2 has a small significant TAC at both TPK and QB (Figure S2(c)). In the SCS, all TACs are insignificant or small for N_2 (Figure S2(b)), but the K_2 response in the Beibu Gulf gauges is exceptionally large (+67 to +175 mm m^{-1}), notable for such a small-magnitude constituent (Figure S2(d)).

The diurnal TACs in HK and the SCS generally exhibit a larger-magnitude and more spatially-coherent response than semidiurnal TACs (Figure 4). Like M_2, the strongest K_1 values in Hong Kong (Fig 4(a)) are seen at QB (+220 ± 15 mm m^{-1}) and TPK (+190 ± 68 mm m^{-1}). In the SCS, the largest magnitude TACs are again found in the Beibu Gulf (+180 to +578 mm m^{-1}), but unlike M_2, all significant TACs are positive in the region (Fig 4(b)), and there is a significantly large TAC at Bintulu. The O_1 results in Hong Kong (Fig 4(c)) and in the SCS (Fig 4(d)) are like the M_2 results, showing positive TACs at QB (+146 ± 11 mm m^{-1}) and TPK (+100 ± 25 mm m^{-1}), and strongly negative TACs west of QB. The O_1 response in the SCS is very similar to K_1, though a negative response is now seen at Xiamen and Shanwei, and a small positive response is seen at Keelung. Phase TACs for K_1 are mainly insignificant in Hong Kong (Figure S3(a)), and O_1 phase TACs (Figure S3(c)) are only significant at QB. In the SCS, strong positive phase TACs are seen at Shanwei and Kaohsiung in both K_1 (Figure S3(b)) and O_1 (Figure S3(d)), and negative phase TACs for K_1 and O_1 are seen in the Beibu Gulf. The minor P_1 tide has a positive TAC at QB and Ma Wan (+71 ± 10 and +65 ± 9 mm m^{-1}; Figure S4(a)), and results are coherent throughout the rest of the SCS, with positive responses seen in the Beibu Gulf of + 50 to +153 mm m^{-1}, and all other locations having negative responses of -19 to -55 mm m^{-}(Fig S4(b)). The results for Q_1 are mixed in Hong Kong (Figure S4(c)), with a positive TAC at QB, a negative TAC at Kwai Chung and Chi Ma Wan. The Q_1 TACs are insignificant at all stations in the SCS (Figure S4(d)).

3.2 Change in the highest astronomical tide (δ-HAT)

The TACs are widely observed in Hong Kong and across the SCS. Conversely, the δ-HATs (Figure 5) are only of significance at discrete locations. In Hong Kong, five stations exhibit significant δ-HAT_4 values (Fig 5(a)), with QB and TPK having very large positive magnitudes (+665 ± 85 mm m^{-1} and +612 ± 210 mm m^{-1}, respectively), and Shek Pik having a lesser magnitude of +138 ± 47 mm m^{-1}. Conversely, Ma Wan and Chi Ma Wan exhibit moderate negative δ-HAT_4 values, (~ -100 mm m^{-1}). The same five gauges are significant for the δ-HAT$_8$ determinations (Fig 5(c)), though the overall magnitudes are larger (e.g., +834 ± 108 mm m^{-1} at QB and +797 ± 139 mm m^{-1} at TPK). In the SCS, the δ-HAT$_4$ determinations are extraordinarily large in the Beibu Gulf, with magnitudes of +813 to +1405 mm m^{-1} (Figure 5(b)), and the δ-HAT$_8$ values are even larger; ~ 20% larger at Haikou and Dongfang, and at Beihei, nearly 60% larger, showing a positive change in tidal range of > 2 meters for a 1-meter sea-level fluctuation (Figure 5(d)). Elsewhere in the SCS of note, there are very large δ-HAT values seen at Bintulu, though this is mostly due to the very large D$_1$-TACs; the D$_2$ band contributes very little to the change in tidal range here.

3.3 D$_1$/D$_2$ TACs and OT TACs

The D$_1$/D$_2$ and OT TACs are important in the northern SCS and are less significant in the southern reaches. In Hong Kong, all significant D$_1$/D$_2$ TACs results are positive (Figure 6(a)), and at most locations the correspondence is nearly 1-to-1 (e.g., QB; +1.08 ± 0.05, TPK; +1.01 ± 0.04, TMW; +1.04 ± 0.20), indicating that a change in D$_1$ can yield a nearly-identical magnitude change in D$_2$, and vice-versa. Smaller magnitude relations are seen in the western areas of the domain (e.g., TBT, +0.37 ± 0.02 and LOP; +0.26 ± 0.05). In the SCS (Figure 6(b)), the strongest relationships are in the Beibu Gulf. At Beihei, the value is nearly 1-to-1 (+1.22 ± 0.03), but at Dongfang, the response is significantly larger than 1 (+2.86 ± 0.19), and at Haikou, the response is less than 1 (+0.61 ± 0.05). Elsewhere, small negative relations are observed near the Taiwan Strait, and large negative relations are seen in the southern SCS.

The OT TACs at half of gauges in Hong Kong (Fig 6(c)) and nearly every gauge in the northern SCS (Fig 6(d)) are significant and negatively correlated. Friction is expected to be important in coastal or harbor regions, and indeed, the strongest correlations are found in semi-enclosed or partially protected areas (e.g., QB and Kwai Chung in and near Victoria Harbor, Tsim Bei Tsui in Shenzhen Bay and TPK in Tolo Harbor). The largest OT TAC in Hong Kong is -3.62 ± 0.99 at QB, meaning that for a negative change in the OT component (which would indicate a reduction of friction) of 1 mm, an increase of 3.62 mm will be seen in the forcing tides. In the SCS, the largest (-5.10 ± 0.15) response is seen at Beihei near the end of the Beibu Gulf. The southern parts of the SCS show no significant relations. The OT variability was also compared to the D$_1$ and D$_2$ bands individually, shown in the supplementary materials (Figure S5), showing that the D$_2$/OT relations are generally more coherent.

3.4 Anomalous tidal events in Hong Kong

We now examine the temporal behavior of the tides in Hong Kong. In Figure 7, the time series of water level spectrum components are shown for QB and TPK, presenting the D_1 band (a), the D_2 band (b), the OT band (c) and mean sea-level (MSL) (d), given as normalized amplitudes with mean values shown in the legends. Some very notable features of these records are clear. At QB, the early part of the record shows nearly constant tidal amplitudes in D_1, while D_2 amplitudes show a slight decrease, and MSL exhibits a slight positive trend. In the mid-1980s, however, both D_1 and D_2 increase drastically until around the year 2003, at which time both tidal bands undergo a rapid decrease of amplitude of ~15%, sustaining this diminished magnitude for about five years before increasing nearly as rapidly. The OT band shows a sustained increase over the historical record, but many of the fluctuations around the trend are anti-correlated to the perturbations in D_1 and D_2, and during the times of diminished major tides, the OTs increase by about +20%. The MSL record is also highly variable at QB, with a nearly flat trend during the increase in tides seen in the 1980s, followed by a strong increase from ~1993-2000, and then a steep decrease concurrent with the time of diminished tides before increasing again. The gauge at TPK shows a similar tidal behavior, though timings and magnitudes are different here. The increase in D_1 and D_2 at TPK in the 1980s is much larger and peaks earlier than QB, reaching a maximum around 1996, and then decreasing around 1998, about five years before the drop at QB. Both locations experience an absolute minimum around 2007 in D_2, but the D_1 minimum at TPK leads the QB minimum by a few years.

We now examine whether these anomalous events are also apparent at other locations in Hong Kong. In Figure 8, the detrended D_2 variability of all gauges is presented as normalized amplitudes. The longest record gauges (QB and TPK) displayed in Figure 7 are shown as heavy lines (blue and red, respectively), with the other gauges shown as thinner lines according to the legend. Horizontal lines indicate a change of ± 5% from the mean. At QB and TPK, the variability during the anomaly is 10-15% of the mean, but such a large anomaly is not clearly apparent elsewhere, and most other gauges show a variation of only a few percent. There does appears to be a similar pattern suggested at TBT, with an increase from ~1988 to 1995, a decrease until 2007, and an increase afterwards; however, this gauge has some large data gaps during this time, so a confident determination of the tidal behavior is unlikely without more observations. Very similar results are seen when considering the D_1

band, shown in the Supplementary material (Figure S6), as well as for the M_2 and K_1 amplitudes (Figures S7 and S8).

3.5 Minor constituent behavior

These anomalies in tidal amplitudes are curious by themselves, however, looking at minor constituents reveals more interesting details. In Figure 9, we present some minor tidal variability as normalized amplitudes for a selection of representative Hong Kong gauges (QB, TPK, TBT, CMW, TMW, MW). The N_2 amplitudes at all Hong Kong stations exhibit a long-period harmonic signal, in phase at all locations, corresponding to the lunar eccentricity cycle of 8.85 years (Fig 9(a)). Typically, this longer-cycle component of the gravitational potential is suppressed in the admittance analyses, but if there is any terrestrial amplification of the N_2 signal, it may be apparent in the post-admittance analyses. There are regular maxima starting from the beginning of the record up to ~2002 at which time a minimum of the cycle is "missed", with the next subsequent minimum being more extreme than all previous minima. This event corresponds with the major anomaly seen in all constituents at QB and TPK. More interestingly, the N_2 signals at Hong Kong tide gauges are all in phase, with a near-simultaneous minimum around 2009. The $2N_2$ tide has a similar gravitational origin as N_2 (Fig 9(b)) and exhibits a similar long-period harmonic signal of ~ 4.425 year (8.85/2 year). Before the anomaly period, the $2N_2$ signal is relatively uncorrelated and noisy, but after ~2000, the spatial coherence of $2N_2$ increases, while the N_2 coherency decreases. After 2009, the harmonic signal is no longer evident in N_2, as there is no clear maximum in ~2013. The M_3 tide, usually small (<5 mm) and noisy in the ocean, is significant at all Hong Kong gauges (~15-25 mm), and also exhibits a ~ 8.85-year signal at all gauges (Fig 9(c)). There is again a large anomaly present at all gauges after the turn of the 21st century, though the M_3 minimum leads the N_2 minimum by a few years due to a phase shift. Another component of the D_3 spectrum, the MO_3 tide, also displays a coherent 8.85-year signal (Fig 9(d)). This tidal constituent is typically thought of as a shallow-water overtide but can also arise via nonlinear interactions between M_2 and O_1.

The spatial coherence of the minor tides is not as clear in the greater SCS. Figure 10 displays the same constituents at selected gauges in the SCS. We use Quarry Bay again (to represent Hong Kong), Xiamen (to represent the Taiwan Strait), Dongfang (to represent the Beibu Gulf), Vung Tau (to represent the central SCS), Sedili (to represent the Gulf of Thailand) and Ishigaki (to represent the Pacific Ocean). The N_2 tide is very strong within the

Taiwan Strait (~350 mm at Xiamen), and of moderate amplitude elsewhere (Fig 10(a)). The long-period harmonic signal is also present at most gauges with a similar relative variability, though Dongfang is more variable and noisy, and no other locations shows such a large relative anomaly as QB circa 2009. The $2N_2$ tide is less coherent regionally than Hong Kong (Fig 10(b)), though the correlations between Vung Tau and Sedili do appear to be slightly better after ~2000. At Xiamen, $2N_2$ has the largest observed magnitude (~ 50 mm), and the ~4.425 yr signal is strong, but opposite in phase to QB. For M_3, the long-period signal is generally not observed to be strong in areas of the SCS away from Hong Kong. However, Xiamen does show a large relatively variable signal, which, like $2N_2$, is opposed in phase to QB. Finally, the MO_3 tide (Fig 10(d)) does not appear to be important away from Hong Kong; there is a signal suggested at Ishigaki, but the mean value is very small (~ 3 mm), and this may be attributed to noise.

3.6 Early correlations vs. modern correlations

From looking at Figures 7 through 10, it is apparent that there is more variability in the later years of the record than in the earlier parts of the record. This suggests the possibility of a recent regime change in the tidal behavior in the Hong Kong and SCS and warrants a closer examination. We compare the correlations of QB with other gauges in Hong Kong and the SCS for both the "historical" and "modern" data sets described above to determine the relevant spatial and temporal scales of tidal variability, including the minor constituents considered in Figures 9 and 10. Correlation values for M_2, K_1, M_3, MO_3, N_2, and $2N_2$ amplitudes are given in Table 4. Table S3 gives the correlations for S_2, O_1, K_2, P_1, Q_1, and MSL. Table entries give two entries for longer gauges who cover both time periods (e.g., QB, TPK, and IG), as well as a few station pairs that are close enough geographically to allow a direct comparison (CMW/CHC and LOP/MW), separated by a "/". Gauges that do not have data during either period will be indicated by a "-". Additionally, the average correlation at all gauges in HK and the SCS are given for both eras, and the better correlation between eras will be indicated by bold text.

Results show that the tidal correlations in the region are generally less significant in the later record than the early record. At Tai Po Kau, all constituents have a strong correlation in early years (+0.63 to +0.83) but show a lesser correlation in later years (+0.16 to +0.60). At Tsim Bei Tsui, however, the correlation is somewhat better in later years for semidiurnal constituents. The comparison of Lok On Pai to Ma Wan shows lesser correlations in later years (+0.06 to +0.76) than in early years (+0.35 to +0.87), and the same situation is seen when comparing Cheung Chau (+0.02 to +0.61) to Chi Ma Wan (+0.34 to +0.69). The average correlations of Hong Kong gauges are lower in later years than in early years; e.g. the M_2 average correlation decreases from +0.62 to +0.28, and K_1 from +0.54 to +0.31. In the SCS, historical M_2 and K_1 average correlations are +0.45 and +0.48, but the modern correlations are much smaller (both ~ +0.17). The N_2 tide is highly correlated to QB in both time periods at nearly all gauges in HK and the SCS, due to the long-period harmonic discussed above, but these correlations have decreased from +0.75 in HK and +0.66 in the SCS to +0.67 and +0.48, respectively. The exception to the pattern of decreasing correlations is the $2N_2$ tide, whose correlations increase in the modern era (+0.59 to +0.86 in HK and +0.29 to 0.41 in the SCS). The M_3 tide is highly correlated to QB at most HK gauges (+0.75 to +0.90) which shows similar correlations in both eras; but in the SCS, the M_3 correlations are only strong near HK at Zhapo, Shawei, and Xiamen (though at Xiamen, the tide is anti-correlated to QB). Finally, The MO_3 tide is highly correlated at all locations in HK (+0.78 to +0.92), having increased slightly in the modern era, but in the SCS is only important very near to HK (Zhapo and Shanwei). These correlation changes confirm what was suggested by Figure 9 and 10.

4. Discussion

4.1 Spatial scales of tidal variability

This survey has identified several varieties of tidal variability in Hong Kong and the SCS that suggest multiple spatial scales of importance. The TAC (Figures 3 and 4) and δ-HAT (Figure 5) results appear to be more important on a local basis, as the strongest responses are mainly concentrated at specific locations (e.g., The Beibu Gulf, QB and TPK). These locations also have significant positive correlations of the four largest tidal amplitudes to a positive MSL fluctuation, and both locations show a negative response (earlier arriving tide) of semidiurnal tidal phases. Other locations show a mixed result. The M_2 response is negative at gauges just west of QB (CHC, CMW, MW) and positive at SP, with a similar pattern seen for the O_1 and Q_1 amplitude TACs. Conversely, the K_1 TAC results are generally positive. Minor constituent TACs are generally unimportant in Hong Kong, but TPK is more sensitive to the semidiurnal minor tides, while QB tends to be more sensitive to the diurnal band. At both QB and TPK, the positive reinforcements of individual tidal fluctuations lead to very large δ-HAT_4 and δ-HAT_8 values, though large negative δ-HAT_4 and δ-HAT_8 values are seen near to QB at CMW and MW. The spatial connections in the semi-enclosed center harbor regions suggest a connected mechanism; this area is where the majority of recent Hong Kong coastal reclamation projects have occurred, including the construction of a new island for an airport, shipping channel deepening and other coastal morphology changes. Such changes in water depth and coastal geometry strongly suggest a relation to frictional or resonance changes. The TACs in the Beibu Gulf are strongly positive for most constituents, and the δ-HATs are even larger than those seen at Hong Kong. Away from Hong Kong and the northern SCS, TAC and δ-HATs are of less significance.

The D_1/D_2 TAC relations (Figures 6 (a) and (b)) are a more regionally-relevant phenomenon, being significant nearly everywhere in Hong Kong and in the northwest and north-central SCS, and less significant in the Taiwan Strait and the southern SCS. The majority of significant D_1/D_2 TACs are positive, with most being nearly 1-to-1 (i.e., a ~1-mm change in D_1 will yield a ~1-mm change in D_2), confirmed by the close similarity of tidal behavior of the D_1 and D_2 tidal bands in Hong Kong (e.g., Figure 7 and Figure 8). This aspect of tidal variability in Hong Kong is likely related to the dynamics near the Luzon Strait, where large amounts of baroclinic conversion in both D_1 and D_2 tides tend to couple the variabilities (Jan et al., 2007; 2008; Lien et al., 2015). The low-mode baroclinic energy can travel great distances, being enhanced upon arrival at the shelf and leading to the further generation of energy at non-traditional frequencies such as *f* and M_3 (Xie et al., 2008; 2011; 2013).

There are two sub-regional exceptions to the D_1/D_2 correlations. First, the western part of Hong Kong the relationships are markedly less than 1 to 1 (~0.33 to ~0.25 at TBT and LOP, respectively). This may be partially influenced by effects of the Pearl River, which discharges part of its flow along the Lantau Channel. The flow of the river is highly seasonal and ejects a freshwater plume at every ebb tide that varies by prevailing wind conditions and by the spring-neap cycle (Gu et al., 2012; Pan et al, 2014). The plumes may affect turbulence and mixing in the region and can dissipate energy away the tidal bands, which may "decouple" the correlated response of D_1 and D_2. This may also help explain the insignificant value seen at Zhapo just to the west of Hong Kong within the influence of the river. The second sub-region is in the Taiwan Strait. Here, there is a larger amount of semidiurnal baroclinic energy than diurnal, as part of the D_2 wave that enters through the Luzon Strait travels north through the Taiwan Strait to meet the incoming D_2 wave from the East China Sea, leading to a pronounced resonance along the Taiwan coast (though not along the coast of

China, due to the irregular topography of the cross-section. (Jan et al., 2004). However, there is no significant diurnal wave or internal tide in the Taiwan Strait, so the semidiurnal constituents dominate here, and is thus decoupled from the diurnal variability.

The OT TAC results in Hong Kong and the SCS show a generally negative relation (Figure 6 (c) and (d)). The sensitivity of shallow-water overtides (OT) to fluctuations in the forcing tides are most significant at harbor locations and along the southeastern reaches of Hong Kong. In the SCS, OT TACs are most important in the Beibu Gulf and near the Taiwan Strait, further suggesting the importance of friction in these dynamic regions. The strength of forcing tides and shallow-water overtides should both be dependent on the depth and morphology, so such a inverse relationship is to be expected in general. However, the implications of the frictional response can be complex under scenarios of rising sea levels (e.g., Hollemann and Stacey, 2014). For a sea-level rise along a shore with a gently sloping bottom, such as a beach, rising sea levels will inundate more low-lying areas, increasing friction and dissipating energy from the forcing tides. By contrast, harbors are deeper and flat-walled, often deepened further to develop navigation channels or accommodate shipping terminals. For these regions, sea-level rise will decrease friction, as the distance from the bottom will increase without new land areas being inundated, hence, less energy will be dissipated from the forcing tides. This in turn may have indirect effects on the total sea levels in other regions near the deep harbor areas. In either situation, the relations of OTs to forcing tides will be negative. Interestingly, the OT TACs are insignificant in the southern SCS; since these regions are the shallowest in the study domain, they should be subject to large frictional tides, yet they are not correlated to the forcing tides as they are in the northern SCS. This may be at least partly attributable to the dominant importance of seasonal processes in the Gulf of Thailand reported on by Devlin et al. (2018) and may be indicative of the OT TAC relations in the northern SCS being more closely related to baroclinic activity than water depth, since baroclinic energy is less important in very shallow regions.

4.2 Effects of regional tidal variability on local variability

The presence of strong M_3 and MO_3 tides at most gauges in Hong Kong (Fig 9) indicates a connection to the dynamics at the shelf where significant D_3 energy has been observed (Xie et al., 2008). The N_2 tide with its typical ~8.85 yr periodicity is largest in the Taiwan Strait, but closer to Luzon and elsewhere in the SCS, N_2 is much smaller. This suggests that the source of the long-period signal in M_3 and MO_3 is the N_2 energy originating in the Taiwan Strait. The N_2 wave may couple with the incoming D_1 and D_2 energy from Luzon at the northern SCS shelf and may intensify PSI and triad interactions. The M_3 and MO_3 signals are likely initially generated near the shelf, and then may be enhanced by N_2 energy from the Taiwan Strait which imparts the long-period modulation to the D_3 band, leading to coherent D_3 signals with long-period modulations observable in Hong Kong. A resonance in M_3 has been observed before on the shelf near Brazil in the south Atlantic (Huthnance, 1980), demonstrating that a large M_3 can result from a combination of an "organ pipe" quarter wave resonance from the tide that leads to high amplitudes at the shore (Webb, 1976), and a half-wave transverse resonance that enhances the tides at the edge of the shelf. Such a mechanism is also possible near Hong Kong, which is at a similar latitude as Brazil, and the shelf in the SCS near Hong Kong has similar depth, width, and slope characteristics as the Brazil shelf. This hypothesis is further supported by noticing that the long-period modulation is strongest in the Taiwan Strait and northern shelf region but diminishes further away (Fig 10). In the Beibu Gulf and the southern SCS, the N_2 variation is almost nonexistent, and the M_3 signal is much smaller. Outside the SCS in the Pacific (Ishigaki), the M_3 tide is virtually nonexistent, with no significant periodicity seen.

The usually insignificant $2N_2$ tide is also interesting, being more spatially coherent than N_2 in Hong Kong after ~2000, before the anomalous event (Fig 9(b)). This suggests that the anomaly could be related to a resonance shift due to the combination of rising sea-levels and the anthropogenically modified coastal morphology. Since the N_2 and $2N_2$ frequencies are close (within 2%), is it possible that the extensive changes to the coastal morphology have shifted the dominant resonance by a similar amount, yielding the anomaly event as a harmonic adjustment to new forcing conditions. It may alternatively be related to a regional change in the SCS (e.g., rising MSL or increased stratification due to upper-ocean warming). However, since data coverage is sparse in the SCS, and few locations allow direct comparisons of "before and after", any conclusions based on this limited data would be hasty. Local and regional models may help to determine which spatial scale is most relevant.

Hong Kong has had a long history of land reclamation to accommodate an ever-growing infrastructure and population, including the building of a new airport island (Chep Lap Kok), land connections and from the Kowloon Peninsula to Stonecutters' Island and channel deepening to accommodate container terminals, and many bridges, tunnels, and "new cities", built on reclaimed land (e.g., Tai Po and Tseung Kwan O). All of these may have changed the resonance and/or frictional properties of the region. Tai Po Kau has also seen some land reclamation efforts, such as Science Park, that have changed the coastal morphology. Both locations also show coherent D_1/D_2 and OT TACs, as well as having the largest δ-HATs, and the largest tidal anomalies in the 2000s. Other locations in Hong Kong did not show such extreme variations, so these variations appear to be amplified in harbor areas. Decreases in friction associated with sea-level rise in the SCS may lead to higher forcing tides, and those changes may also be amplified by the close correlations of D_1 and D_2 variability or local harbor development which may further decrease local friction. Hence, a small change in friction due to a small sea-level change may induce a significant change in tidal amplitudes. The positive reinforcement of multiple tides correlated with regional sea-level adjustments may amplify the risks of coastal inundation and coastal flooding, as evidenced by the gauges that had the largest δ-HAT values.

4.3 Limitations of this study and future steps

The inventory of tide gauges provided by HKO and the HKMD has revealed new dynamics and spatial connectivity in the area. However, some gauges are of short length and/or riddled with data gaps, making a full analysis of the area problematic. For example, the Tsim Bei Tsui (TBT) gauge covers a long period, but there are significant gaps in the record, which complicates our analysis. This gauge is located within a harbor region (Deep Bay), bordered to the north by Shenzhen, PRC, which has also grown and developed its coastal infrastructure in past decades, therefore, one might expect similar dynamics are was seen at QB and TPK. While there were significant OT TACs, and D_1/D_2 correlations at TBT, no significant TACs or δ-HATs were observed. The large anomalies seen at QB and TPK around 2000 are suggested by the data at TBT, but some of the missing data corresponds to this time. Without more data or observations, no answers can be concluded about this location at the present time. However, future studies will examine this region via remote sensing and *in-situ* data to better understand the tidal behavior in this area, since the Deep Bay region is highly ecologically sensitive, being populated by extensive mangrove forests which may be disturbed by rapidly changing sea levels (Zhang et al., 2018), so accurate determination of future sea levels is of utmost importance to the vitality of these important ecosystems.

Furthermore, there is only limited historical data available in the rest of the SCS, most of it having not been updated in 20 years. This complicates efforts to understand the full spatial and temporal extent of the tidal variability in the greater SCS region. A caveat is also made about the very large TACs and δ HATs observed in the Beibu Gulf; these are likely due to the sensitive resonance in the Gulf, and it is unlikely that such large-magnitude changes will remain linear over such large MSL fluctuations (i.e., it violates the "small-amplitude" assumption taken above). Yet, the behavior in the region is still worthy of future study. Another limitation comes from the nature of the harmonic analysis technique used (R_T_TIDE) which only resolves energy at discrete tidal frequencies. This will not be able to identify tidal energy at the local (latitude-dependent) inertial frequency, *f* (at Hong Kong, T_f ~ 31.625 hr), which may be a significant component of the energy cascade (Xie et al., 2008; 2011;2013; Chinn et al., 2012). It is also likely that the M_1 tide is part of the cascade, yet this tide was below the noise limit at all gauges analyzed here. However, since the M_1 interactions are an intermediate step that transfers energy to M_3 (i.e., M_2 to M_1, then to M_3 via $M_2 + M_1$), this energy is high-frequency and not detectable at the yearly-analyzed scale. Finally, there are only surface observations available (i.e., tide gauges), though the tidal velocities are also variable at depth. The installation of current profilers at inland and offshore locations near Hong Kong could provide beneficial observations of the three-dimensional dynamics, could reveal the presence of energy at lesser frequencies such as M_1 and *f* as well as being able to separate the baroclinic component of the tides. Previous current profiler observations in the Hong Kong waters are currently being analyzed, to be presented in a future study. Finally, the tidal variability could be better explored via utilization of analytical and numerical models. This is beyond the scope of the current observational study but is the subject of an ongoing project.

5. Conclusions

This study has presented new information about the tidal variability in Hong Kong, based on observations of a set of historical and modern tide gauges in Hong Kong and in the South China Sea. The observed dynamics support the hypothesis that the changes are due to multiple processes and are best described as an amplification of the local (Hong Kong) tidal response to changes in the prevailing regional (SCS) tidal patterns, which may have been enhanced by local harbor changes and land reclamation. The D_1/D_2 and OT TACs, on the other hand, are more likely due to the internal tide dynamics near the Luzon Strait which are enhanced at the shelf; this may influence the tidal behavior in other parts of the SCS and may also explain the large spatial scale of these correlations, as well as explaining the presence of M_3. The large TACs and δ HATs in Hong Kong and the anomalous events in tidal amplitudes seen at the Quarry Bay and Tai Po Kau gauges are likely due to a combination of changing resonance and friction induced by coastal improvement projects which may amplify the regional D_1/D_2 and OT TACs in harbor regions. These anomalies also suggest that a regime change in tidal resonance has occurred, with the effect being most pronounced at gauges in semi-enclosed harbors where all tidal components are strongly modulated via the conservation of the D_1/D_2 ratios. A shift in the tidal regime is further suggested by the less significant spatial correlations of most tidal components (except $2N_2$) observed in recent years as compared to historical eras.

Overall, the tidal variability seen in Hong Kong may have significant impacts on the future of total sea-levels in the region. Short-term inundation events, such as nuisance flooding, may be amplified under scenarios of higher sea-levels that lead to corresponding changes in the tides, as evidenced by the strong D_1/D_2 and OT connections and very large TACs which may amplify small changes in water levels or reductions in friction due to harbor improvements. It is probable that changes in harbor geometry have influenced tidal evolution in Hong Kong as a cumulative effect of all projects. Future studies will perform simple analytical models as well as high resolution three-dimensional models to simulate changing coastlines under a variety of sea-level, tidal forcing, and anthropogenic change scenarios (historical and future) to better understand the tidal dynamics in Hong Kong at the local scale (e.g., how much morphological change in a harbor region would be needed to shift the dominant resonance from N_2 to $2N_2$), conditions that allow or enhance PSI or resonant triad interactions, and the utilization satellite-derived tidal observations and models in the South China Sea to better understand the dynamics at the regional scale, particularly the D_1/D_2 ratios, and the M_3 prevalence in the SCS.

Code availability All code employed in this study was developed using MATLAB, version R2011B. All code and methods can be provided upon request.

Data Availability The data used in this study from the Hong Kong Observatory (HKO; www.hko.gov.hk) and the Hong Kong Marine Department (HKMD; www.mardep.gov.hk/en/home.html) was provided upon request, discussion of intentions of use, and permission from the appropriate agency supervisors. Data used from the University of Hawaii Sea Level Center (UHSLC; www.uhslc.soest.hawaii.edu) is publicly available.

Author Contributions ATD did all analyses, figures, tables, the majority of writing, and complied the manuscript. JP provided editing, insight, guidance, and direction to this study. HL provided critical and helpful input.

Competing Interests The authors declare they have no competing interest.

Acknowledgements This work is supported by The National Basic Research Program of China (2015CB954103), the National Natural Science Foundation of China (project 41376035), the General Research Fund of Hong Kong Research Grants Council (RGC) (CUHK 402912 and 403113), the Hong Kong Innovation and Technology Fund under the grants (ITS/259/12 and ITS/321/13), and the direct grants of the Chinese University of Hong Kong.

FIGURE CAPTIONS:

Figure 1 Tide gauge locations in Hong Kong used in this study. Green markers indicate active gauges provided by the Hong Kong Observatory (HKO), light blue markers indicate gauges provided by the Hong Kong Marine Department (HKMD), and red markers indicate historical gauges once maintained by HKO that are no longer operational.

Figure 2 Tide gauge locations in the South China Sea (SCS). All tide gauge data is provided by the University of Hawaii Sea Level Center; green markers indicate actively recording and updated tide gauges, and red markers indicate historical gauges that have not been publicly updated since 1997.

Figure 3 Semidiurnal tidal anomaly correlations (TACs) of detrended M_2 amplitude to detrended MSL in (a) Hong Kong, (b) the South China Sea, and of detrended S_2 amplitude to detrended MSL in (c) Hong Kong, and (d) the South China Sea. Red markers indicate positive TACs and blue indicates negative TACs, with the marker size showing the relative magnitude according to the legend. Black marks indicate insignificant TACs. Map backgrounds in (b) and (d) show mean tidal amplitudes over the period of 1993-2014 (color scale, meters) and phases (solid lines, 30° increment), taken from the ocean tidal model of TPXO7.2, (Egbert and Erofeeva, 2002, 2010).

Figure 4 Diurnal tidal anomaly correlations (TACs) of detrended K_1 amplitude to detrended MSL in (a) Hong Kong, (b) the South China Sea, and of detrended O_1 amplitude to detrended MSL in (c) Hong Kong, and (d) the South China Sea. Red markers indicate positive TACs and blue indicates negative TACs, with the marker size showing the relative magnitude according to the legend. Black marks indicate insignificant TACs. Map backgrounds in (b) and (d) show mean tidal amplitudes over the period of 1993-2014 (color scale, meters) and phases (solid lines, 30° increment), taken from the ocean tidal model of TPXO7.2, (Egbert and Erofeeva, 2002, 2010).

Figure 5 Results of the δ-HAT_4 determinations, the correlation of detrended ($M_2 + S_2 + K_1 + O_1$) to detrended MSL in Hong Kong (a) and the SCS (b), and results of the δ-HAT_8 determinations, the correlation of detrended ($M_2 + S_2 + N_2 + K_2 + K_1 + O_1 + P_1 + Q_1$) to detrended MSL in Hong Kong (c) and the SCS (d). Red markers indicate positive TACs and blue indicates negative TACs, with the marker size showing the relative magnitude according to the legend. Black marks indicate insignificant TACs.

Figure 6 Results of the D_1/D_2 TACs, the correlation of detrended D_2 ($M_2 + S_2 + N_2 + K_2$) to detrended D_1 ($K_1 + O_1 + P_1 + Q_1$) in Hong Kong (a) and the SCS (b), and results of the OT TACs, the correlation of detrended ($D_1 + D_2$) to detrended OT($M_4 + M_6 + MK_3 + MO_3 + MS_4 + MN_4 + S_4$) in Hong Kong (c) and the SCS (d). Red markers indicate positive TACs and blue indicates negative TACs, with the marker size showing the relative magnitude according to the legend. Black marks indicate insignificant TACs.

Figure 7 Time series of water level spectrum components at the Quarry Bay (QB; blue) and Tai Po Kau (TPK; red) tide gauges in Hong Kong, showing the D_1 band (a), the D_2 band (b), the OT band (c) and mean sea level (MSL) (d). Components are plotted as a function of normalized amplitudes to show relative variability, with mean values given in the legend.

Figure 8 Time-series of the detrended D_2 water level spectrum component at all tide gauges in Hong Kong, plotted as a normalized amplitude to show relative variability, with mean values given in the legend. Each gauge is indicated by color according to the legend, with the QB (solid blue) and TPK (solid red) gauges shown as heavier lines. Horizontal dotted lines indicate the ±5% variational band relative to the mean amplitude.

Figure 9 Minor constituent variability at selected Hong Kong gauges. N_2 is shown in (a), $2N_2$ in (b), M_3 in (c) and MO_3 in (d). All quantities are plotted as normalized amplitudes to show relative variability, with mean values given in the legends at the right.

Figure 10 Minor constituent variability at selected South China Sea gauges. N_2 is shown in (a), $2N_2$ in (b), M_3 in (c) and MO_3 in (d). All quantities are plotted as normalized amplitudes to show relative variability, with mean values given in the legends at the right.

FIGURES

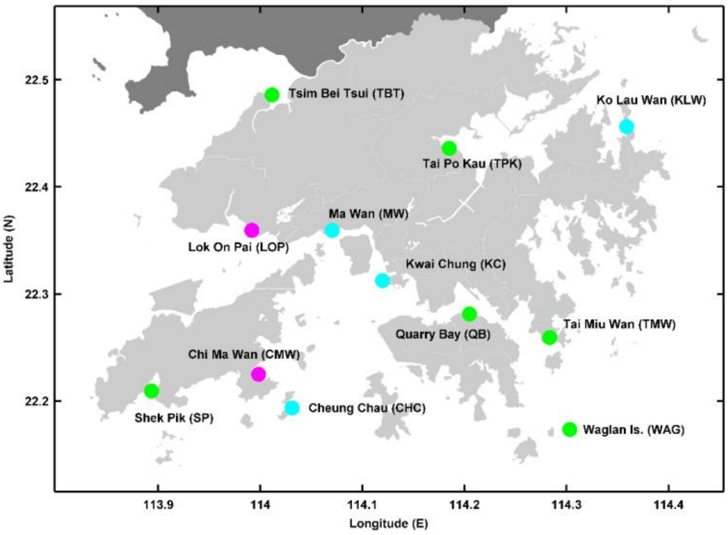

Figure 1 Tide gauge locations in Hong Kong used in this study. Green markers indicate active gauges provided by the Hong Kong Observatory (HKO), light blue markers indicate gauges provided by the Hong Kong Marine Department (HKMD), and red markers indicate historical gauges once maintained by HKO that are no longer operational.

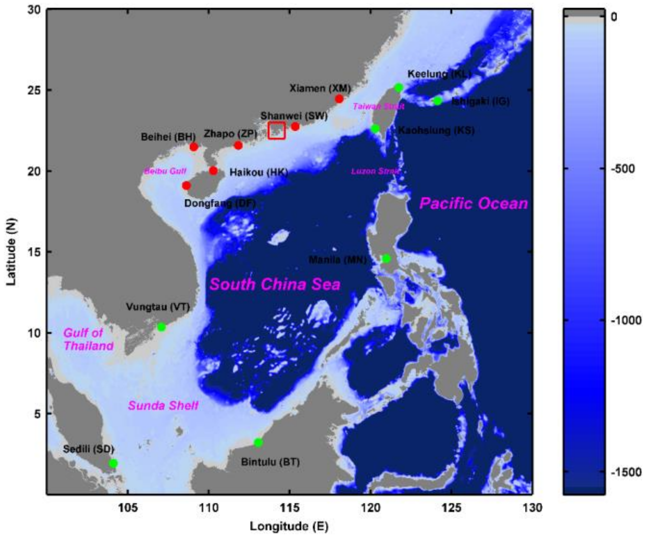

~~**Figure 2** Tide gauge locations in the South China Sea (SCS). All tide gauge data is provided by the University of Hawaii Sea Level Center; green markers indicate actively recording and updated tide gauges, and red markers indicate historical gauges that have not been publicly updated since 1997.~~

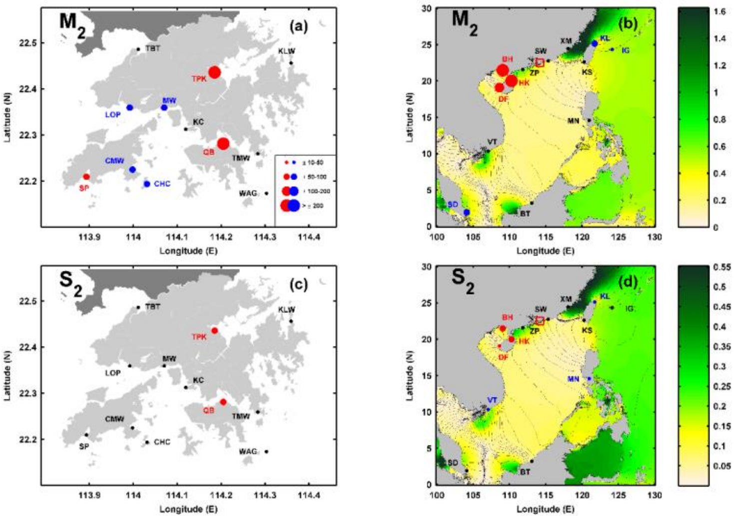

Figure 3 Semidiurnal tidal anomaly correlations (TACs) of detrended M_2 amplitude to detrended MSL in (a) Hong Kong, (b) the South China Sea, and of detrended S_2 amplitude to detrended MSL in (c) Hong Kong, and (d) the South China Sea. Red markers indicate positive TACs and blue indicates negative TACs, with the marker size showing the relative magnitude according to the legend. Black marks indicate insignificant TACs. Map backgrounds in (b) and (d) show mean tidal amplitudes over the period of 1993-2014 (color scale, meters) and phases (solid lines, 30° increment), taken from the ocean tidal model of TPXO7.2, (Egbert and Erofeeva, 2002, 2010).

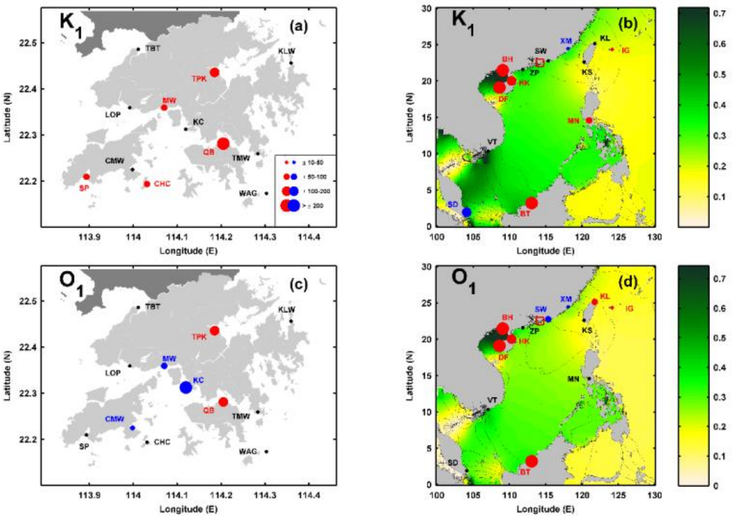

Figure 4 Diurnal tidal anomaly correlations (TACs) of detrended K_1 amplitude to detrended MSL in (a) Hong Kong, (b) the South China Sea, and of detrended O_1 amplitude to detrended MSL in (c) Hong Kong, and (d) the South China Sea. Red markers indicate positive TACs and blue indicates negative TACs, with the marker size showing the relative magnitude according to the legend. Black marks indicate insignificant TACs. Map backgrounds in (b) and (d) show mean tidal amplitudes over the period of 1993-2014 (color scale, meters) and phases (solid lines, 30° increment), taken from the ocean tidal model of TPXO7.2, (Egbert and Erofeeva, 2002, 2010).

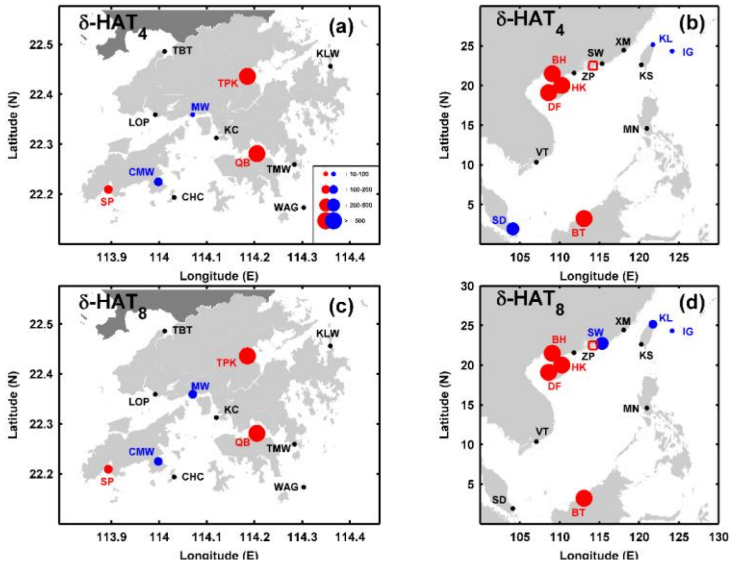

~~**Figure 5** Results of the δ-HAT$_4$ determinations, the correlation of detrended ($M_2 + S_2 + K_1 + O_1$) to detrended MSL in Hong Kong (a) and the SCS (b), and results of the δ-HAT$_8$ determinations, the correlation of detrended ($M_2 + S_2 + N_2 + K_2 + K_1 + O_1 + P_1 + Q_1$) to detrended MSL in Hong Kong (c) and the SCS (d). Red markers indicate positive TACs and blue indicates negative TACs, with the marker size showing the relative magnitude according to the legend. Black marks indicate insignificant TACs.~~

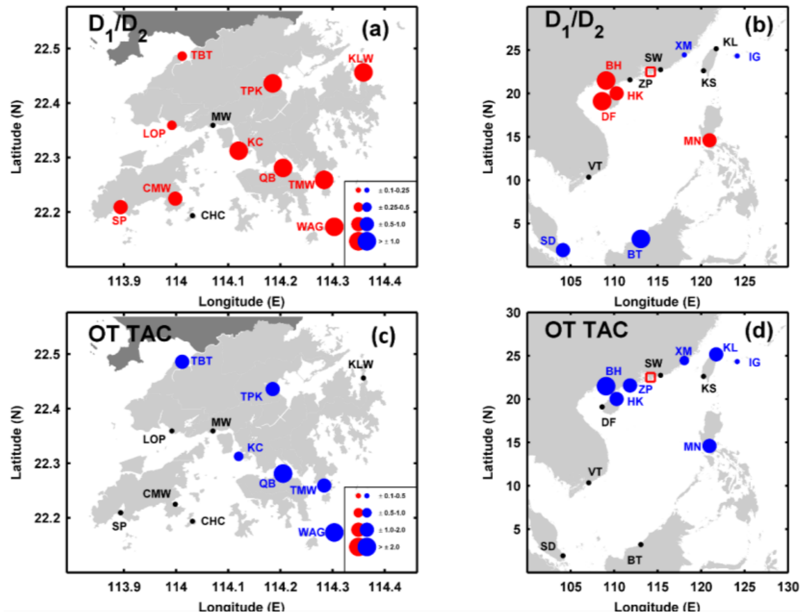

Figure 6 Results of the D_1/D_2 TACs, the correlation of detrended D_2 ($M_2 + S_2 + N_2 + K_2$) to detrended D_1 ($K_1 + O_1 + P_1 + Q_1$) in Hong Kong (a) and the SCS (b), and results of the OT TACs, the correlation of detrended ($D_1 + D_2$) to detrended OT($M_4 + M_6 + MK_3 + MO_3 + MS_4 + MN_4 + S_4$) in Hong Kong (c) and the SCS (d). Red markers indicate positive TACs and blue indicates negative TACs, with the marker size showing the relative magnitude according to the legend. Black marks indicate insignificant TACs.

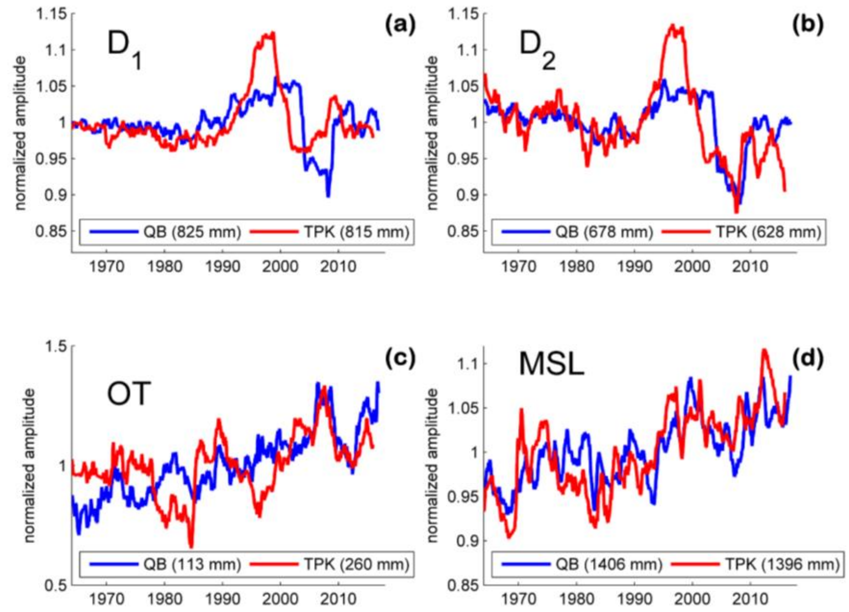

Figure 7. Time series of water level spectrum components at the Quarry Bay (QB; blue) and Tai Po Kau (TPK; red) tide gauges in Hong Kong, showing the D_1 band (a), the D_2 band (b), the OT band (c) and mean sea level (MSL) (d). Components are plotted as a function of normalized amplitudes to show relative variability, with mean values given in the legend.

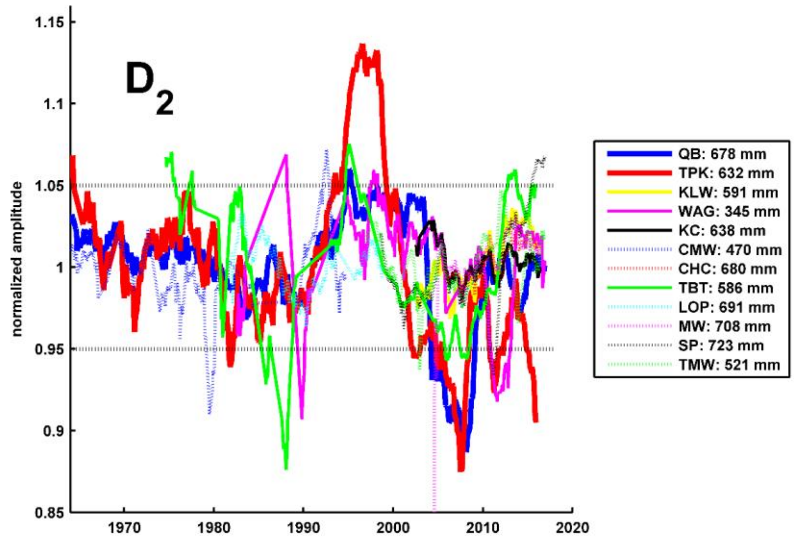

Figure 8 Time-series of detrended D_2 at all tide gauges in Hong Kong, plotted as a normalized amplitude to show relative variability, with mean values given in the legend. Each gauge is indicated by color according to the legend, with the QB (solid blue) and TPK (solid red) gauges shown as heavier lines. Horizontal dotted lines indicate the ±5% variational band relative to the mean amplitude.

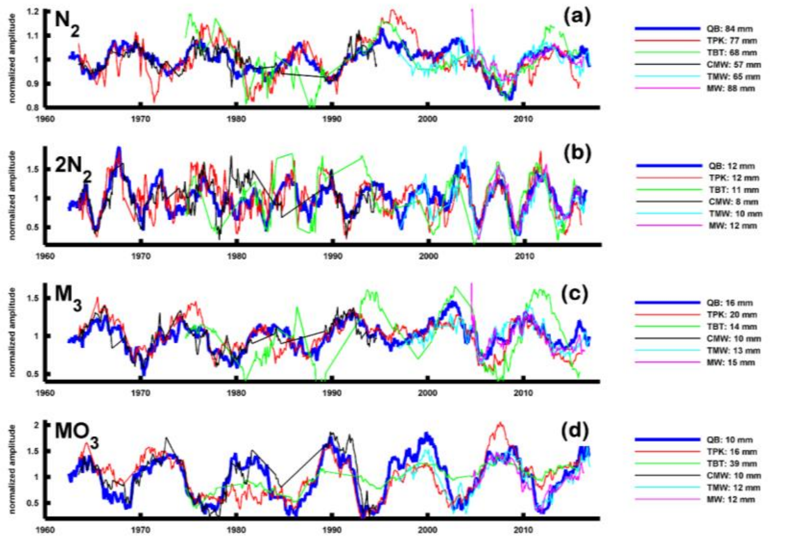

Figure 9 Minor constituent variability at selected Hong Kong gauges. N_2 is shown in (a), $2N_2$ in (b), M_3 in (c) and MO_3 in (d). All quantities are plotted as normalized amplitudes to show relative variability, with mean values given in the legends at the right.

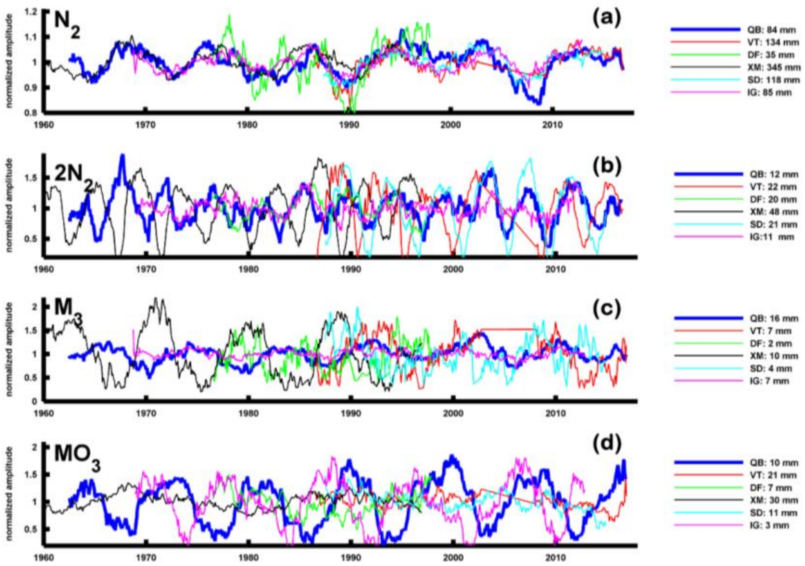

Figure 10 Minor constituent variability at selected South China Sea gauges. N_2 is shown in (a), $2N_2$ in (b), M_3 in (c) and MO_3 in (d). All quantities are plotted as normalized amplitudes to show relative variability, with mean values given in the legends at the right.

REFERENCES:

Alford, M. H. (2008). Observations of parametric subharmonic instability of the diurnal internal tide in the South China Sea. *Geophysical Research Letters*, 35, L15602. doi:10.1029/2008GL034720

Amin, M. (1983). On perturbations of harmonic constants in the Thames Estuary. Geophysical Journal of the Royal Astronomical Society. *73*(3): 587-603. doi:10.1111/j.1365-246X.1983.tb03334.x

Arbic, B.K., Karsten, R.H., Garrett, C. (2009). On tidal resonance in the global ocean and the back-effect of coastal tides upon open-ocean tides. *Atmosphere-Ocean 47*(4), 239–266. doi:10.3137/OC311.2009

Arns, A., Dangendorf, S., Jensen, J., Bender, J., Talke, S.A., & Pattiaratchi, C. (2017). Sea-level rise induced amplification of coastal protection design heights. *Nature: Scientific Reports,7*, 40171. doi:10.1038/srep40171

Bowen, A. J., & Gray, D. A. (1972). The tidal regime of the River Thames; long-term trends and their possible causes. *Phil. Trans. R. Soc. Lond. A, 272*(1221), 187-199. doi:10.1098/rsta.1972.0045

Buchanan, M. K., Oppenheimer, M., & Kopp, R. E. (2017). Amplification of flood frequencies with local sea level rise and emerging flood regimes. *Environmental Research Letters, 12*(6), 064009. doi:10.1088/1748-9326/aa6cb3.

Carter, G.S. and M.C. Gregg (2006), Persistent near-diurnal internal waves observed above a site of M_2 barotropic-to-baroclinic conversion. *Journal of physical oceanography*, *36*(6), 1136-1147. doi:10.1175/JPO2884.1

Cartwright, D.E., & Tayler, R.J. (1971). New computations of the tide-generating potential. *Geophys. Journal of the Royal Astronomical Society*, *23*, 45-74. doi: 10.1111/j.1365-246X.1971.tb01803.x

Cartwright, D.E. (1972). Secular changes in the oceanic tides at Brest, 1711–1936. *Geophysical Journal International*, 30(4), 433-449. doi:10.1.1.867.2468

Cartwright, D.E., & Edden, A.C. (1973). Corrected tables of tidal harmonics. *Geophysical Research Letters, 33*, 253-264. doi:10.1111/j.1365-246X.1973.tb03420.x

Chernetsky, A. S., Schuttelaars, H. M., & Talke, S. A. (2010). The effect of tidal asymmetry and temporal settling lag on sediment trapping in tidal estuaries. *Ocean Dynamics*, *60*(5), 1219-1241.. doi: 10.1007/s10236-010-0329-8

Cherqui, F., Belmeziti, A., Granger, D., Sourdril, A., & Le Gauffre, P. (2015). Assessing urban potential flooding risk and identifying effective risk-reduction measures. *Science of the Total Environment*, *514*, 418-425.

Chinn, B. S., Girton, J. B., & Alford, M. H. (2012). Observations of internal waves and parametric subharmonic instability in the Philippines archipelago. *Journal of Geophysical Research: Oceans*, *117*(C5). doi:10.1029/2011JC007392

Church, J. A., & White, N. J. (2006). A 20th century acceleration in global sea-level rise. *Geophysical research letters*, *33*(1). doi:10.1029/2005GL024826

Church, J. A., & White, N. J. (2011). Sea-level rise from the late 19th to the early 21st century. *Surveys in geophysics*, *32*(4-5), 585-602. doi 10.1007/s10712-011-9119-1

Colosi, J. A., & Munk, W. (2006). Tales of the venerable Honolulu tide gauge. *Journal of physical oceanography*, *36*(6), 967-996. doi:10.1175/JPO2876.1

Craik, A.D.D. (1985). Wave Interactions and Fluid Flows. Cambridge Univ. Press, Cambridge, U. K, ISBN: 978-0521368292

Devlin, A. T., Jay, D. A., Talke, S. A., & Zaron, E. (2014). Can tidal perturbations associated with sea level variations in the western Pacific Ocean be used to understand future effects of tidal evolution? *Ocean Dynamics*, *64*(8), 1093-1120. doi:10.1007/s10236-014-0741-6

Devlin, A.T., (2016). On the variability of Pacific Ocean Tides at seasonal to decadal time scale: Observed vs. modelled. *PhD thesis*, Portland State University

Devlin, A. T., Jay, D. A., Zaron, E. D., Talke, S. A., Pan, J., & Lin, H. (2017). Tidal variability related to sea level variability in the Pacific Ocean. *Journal of Geophysical Research: Oceans*, *122*(11), 8445-8463. doi:10.1002/2017JC013165

Devlin, A. T., Jay, D. A., Talke, S. A., Zaron, E. D., Pan, J., & Lin, H. (2017). Coupling of sea level and tidal range changes, with implications for future water levels. *Scientific Reports*, *7*(1), 17021. doi:10.1038/s41598-017-17056-z

Devlin, A. T., Zaron, E. D., Jay, D. A., Talke, S. A., & Pan, J. (2018). Seasonality of Tides in Southeast Asian Waters. *Journal of Physical Oceanography*. doi: 10.1175/JPO-D-17-0119.1 (accepted Feb. 2018)

Domingues, C. M., Church, J. A., White, N. J., Gleckler, P. J., Wijffels, S. E., Barker, P. M., & Dunn, J. R. (2008). Improved estimates of upper-ocean warming and multi-decadal sea-level rise. *Nature*, *453*(7198), 1090. doi:10.1038/nature07080

Egbert, G. D., & Erofeeva, S. Y. (2002). Efficient inverse modeling of barotropic ocean tides. *Journal of Atmospheric and Oceanic Technology*, *19*(2), 183-204. doi: 10.1175/1520-0426(2002)019<0183: EIMOBO>2.0.CO; 2

Egbert, G. D. & Erofeeva, S. Y. (2010). OTIS (OSU Tidal Inversion Software) TPXO7.2. College of Oceanic and Atmospheric Sciences, Oregon State University, Corvallis, Oregon, http://volkov.oce.orst.edu/tides/otis.html

Haigh, I. D., Wijeratne, E. M. S., MacPherson, L. R., Pattiaratchi, C. B., Mason, M. S., Crompton, R. P., & George, S. (2014). Estimating present day extreme water level exceedance probabilities around the coastline of Australia: tides, extra-tropical storm surges and mean sea level. *Climate Dynamics*, *42*(1-2), 121-138. doi: 10.1007/s00382-012-1652-1

Familkhalili, R., & Talke, S. A. (2016). The effect of channel deepening on tides and storm surge: A case study of Wilmington, NC. *Geophysical Research Letters*, *43*(17), 9138-9147. doi:10.1002/2016GL069494

Fang, G., Kwok, Y. K., Yu, K., & Zhu, Y. (1999). Numerical simulation of principal tidal constituents in the South China Sea, Gulf of Tonkin and Gulf of Thailand. *Continental Shelf Research*, *19*(7), 845-869. doi: 10.1016/S0278-4343(99)00002-3

Feng, X., Tsimplis, M. N., & Woodworth, P. L. (2015). Nodal variations and long-term changes in the main tides on the coasts of China. *Journal of Geophysical Research: Oceans*, *120*(2), 1215-1232. doi:10.1002/2014JC010312

Huthnance, J. M. (1980). On shelf-sea 'resonance' with application to Brazilian M3 tides. *Deep Sea Research Part A. Oceanographic Research Papers*, *27*(5), 347-366. doi:10.1016/0198-0149(80)90031-X

Ip, S.F. and H.G. Wai (1990), *An application of harmonic method to tidal analysis and prediction in Hong Kong*. Royal Observatory.

Korobov, A. S., & Lamb, K. G. (2008). Interharmonics in internal gravity waves generated by tide-topography interaction. *Journal of Fluid Mechanics*, *611*, 61-95. doi:10.1017/S0022112008002449

Jan, S., Chern, C. S., Wang, J., & Chao, S. Y. (2004). The anomalous amplification of M_2 tide in the Taiwan Strait. *Geophysical Research Letters*, *31*(7). doi:10.1029/2003GL019373

Jan, S., Chern, C. S., Wang, J., & Chao, S. Y. (2007). Generation of diurnal K_1 internal tide in the Luzon Strait and its influence on surface tide in the South China Sea. *Journal of Geophysical Research: Oceans*, *112*(C6). doi:10.1029/2006JC004003

Jan, S., Lien, R. C., & Ting, C. H. (2008). Numerical study of baroclinic tides in Luzon Strait. *Journal of Oceanography*, *64*(5), 789. doi:10.1007/s10872-008-0066-5

Jay, D. A. (2009). Evolution of tidal amplitudes in the eastern Pacific Ocean. *Geophysical Research Letters*, *36*(4). doi: 10.1029/2008GL036185

Leffler, K. E., & Jay, D. A. (2009). Enhancing tidal harmonic analysis: Robust (hybrid L1/L2) solutions. *Continental Shelf Research*, *29*(1), 78-88. doi: 10.1016/j.csr.2008.04.011

Li, K. W., & Mok, H. Y. (2012). Long term trends of the regional sea level changes in Hong Kong and the adjacent waters. In *Asian And Pacific Coasts 2011* (pp. 349-359). doi:10.1142/9789814366489_0040

Lien, R. C., Tang, T. Y., Chang, M. H., & d'Asaro, E. A. (2005). Energy of nonlinear internal waves in the South China Sea. *Geophysical Research Letters*, *32*(5). doi:10.1029/2004GL022012

Liu, Q., Xie, X., Shang, X., & Chen, G. (2016). Coherent and incoherent internal tides in the southern South China Sea. *Chinese journal of oceanology and limnology*, *34*(6), 1374-1382. doi:10.1007/s00343-016-5171-5

MacKinnon, J. A., & Winters, K. B. (2005). Subtropical catastrophe: Significant loss of low-mode tidal energy at 28.9°. *Geophysical Research Letters*, *32*(15). doi:10.1029/2005GL023376

Mawdsley, R. J., Haigh, I. D., & Wells, N. C. (2014). Global changes in mean tidal high water, low water and range. *Journal of Coastal Research*, *70*(sp1), 343-348. doi:10.2112/SI70-058.1

McComas, C. H., & Bretherton, F. P. (1977). Resonant interaction of oceanic internal waves. *Journal of Geophysical Research*, *82*(9), 1397-1412. doi:10.1029/JC082i009p01397

Mercier, M. J., Mathur, M., Gostiaux, L., Gerkema, T., Magalhães, J. M., Da Silva, J. C., & Dauxois, T. (2012). Soliton generation by internal tidal beams impinging on a pycnocline: laboratory experiments. *Journal of Fluid Mechanics*, *704*, 37-60. doi:10.1017/jfm.2012.191

Moftakhari, H. R., AghaKouchak, A., Sanders, B. F., Feldman, D. L., Sweet, W., Matthew, R. A., & Luke, A. (2015). Increased nuisance flooding along the coasts of the United States due to sea level rise: Past and future. *Geophysical Research Letters*, *42*(22), 9846-9852. doi:10.1002/2015GL066072

Moftakhari, H. R., AghaKouchak, A., Sanders, B. F., & Matthew, R. A. (2017). Cumulative hazard: The case of nuisance flooding. *Earth's Future*, *5*(2), 214-223. doi:10.1002/2016EF000494

Müller, M., Arbic, B. K., & Mitrovica, J. X. (2011). Secular trends in ocean tides: Observations and model results. *Journal of Geophysical Research: Oceans*, *116*(C5). doi:10.1029/2010JC006387

Müller, M., Cherniawsky, J. Y., Foreman, M. G. G., & Storch, J. S. (2012). Global M_2 internal tide and its seasonal variability from high resolution ocean circulation and tide modeling. *Geophysical Research Letters*, *39*(19). doi:10.1029/2012GL053320

Müller, M. (2012). The influence of changing stratification conditions on barotropic tidal transport and its implications for seasonal and secular changes of tides. *Continental Shelf Research*, *47*, 107-118. doi: 10.1016/j.csr.2012.07.003

Niwa, Y., & Hibiya, T. (2004). Three-dimensional numerical simulation of M_2 internal tides in the East China Sea. *Journal of Geophysical Research: Oceans*, *109*(C4). doi:10.1029/2003JC001923

Pawlowicz, R., Beardsley, B., & Lentz, S. (2002). Classical tidal harmonic analysis including error estimates in MATLAB using T_TIDE. *Computers & Geosciences*, *28*(8), 929-937. doi:10.1016/S0098-3004(02)00013-4

Rasheed, A. S., & Chua, V. P. (2014). Secular trends in tidal parameters along the coast of Japan. *Atmosphere-Ocean*, *52*(2), 155-168. doi:10.1080/07055900.2014.886031

Ray, R. D. (2006). Secular changes of the M_2 tide in the Gulf of Maine. *Continental shelf research*, *26*(3), 422-427. doi: 10.1016/j.csr.2005.12.005

Ray, R. D., & Foster, G. (2016). Future nuisance flooding at Boston caused by astronomical tides alone. *Earth's Future*, *4*(12), 578-587. doi:10.1002/2016EF000423

Ross, A. C., Najjar, R. G., Li, M., Lee, S. B., Zhang, F., & Liu, W. (2017). Fingerprints of Sea Level Rise on Changing Tides in the Chesapeake and Delaware Bays. *Journal of Geophysical Research: Oceans*, *122*(10), 8102-8125. doi:10.1002/2017JC012887

Teoh, S. G., Ivey, G. N., & Imberger, J. (1997). Laboratory study of the interaction between two internal wave rays. *Journal of Fluid Mechanics*, *336*, 91-122. doi:10.1017/S0022112096004508

Vellinga, N. E., Hoitink, A. J. F., van der Vegt, M., Zhang, W., & Hoekstra, P. (2014). Human impacts on tides overwhelm the effect of sea level rise on extreme water levels in the Rhine–Meuse delta. *Coastal Engineering*, *90*, 40-50. doi: 10.1016/j.coastaleng.2014.04.005

Webb, D. J. (1976, January). A model of continental-shelf resonances. In *Deep Sea Research and Oceanographic Abstracts* (Vol. 23, No. 1, pp. 1-15). Elsevier. doi:10.1016/0011-7471(76)90804-4

Woodworth, P. L. (2010). A survey of recent changes in the main components of the ocean tide. *Continental Shelf Research*, *30*(15), 1680-1691. doi: 10.1016/j.csr.2010.07.002

Xie, X. H., Chen, G. Y., Shang, X. D., & Fang, W. D. (2008). Evolution of the semidiurnal (M2) internal tide on the continental slope of the northern South China Sea. *Geophysical Research Letters*, *35*(13). doi:10.1029/2008GL034179

Xie, X. H., Shang, X. D., van Haren, H., Chen, G. Y., & Zhang, Y. Z. (2011). Observations of parametric subharmonic instability-induced near-inertial waves equatorward of the critical diurnal latitude. *Geophysical Research Letters*, *38*(5). doi:10.1029/2010GL046521

Xie, X., Shang, X., Haren, H., & Chen, G. (2013). Observations of enhanced nonlinear instability in the surface reflection of internal tides. *Geophysical Research Letters*, *40*(8), 1580-1586. doi:10.1002/grl.50322

Xing, J., & Davies, A. M. (2002). Processes influencing the non-linear interaction between inertial oscillations, near inertial internal waves and internal tides. *Geophysical Research Letters*, *29*(5). doi:10.1029/2001GL014199

Zaron, E. D., & Jay, D. A. (2014). An analysis of secular change in tides at open-ocean sites in the Pacific. *Journal of Physical Oceanography*, *44*(7), 1704-1726. doi:10.1175/JPO-D-13-0266.1

Zhang, H., Wang, T., Liu, M., Jia, M., Lin, H., Chu, L. M., & Devlin, A. T. (2018). Potential of Combining Optical and Dual Polarimetric SAR Data for Improving Mangrove Species Discrimination Using Rotation Forest. *Remote Sensing*, *10*(3), 467. doi: 10.3390/rs10030467

Zu, T., Gan, J., & Erofeeva, S. Y. (2008). Numerical study of the tide and tidal dynamics in the South China Sea. *Deep Sea Research Part I: Oceanographic Research Papers*, *55*(2), 137-154. doi: 10.1016/j.dsr.2007.10.007

TABLES:

Table 1 Metadata for all tide gauge locations, giving latitude/longitude, and star year/end year of data analyzed. Except where indicated by country code, all locations are located in the People's Republic of China (PRC). The solid horizontal line demarcates Hong Kong and South China Sea tide gauges.

Station	*Latitude*	*Longitude*	*Start Year*	*End Year*
Quarry Bay (QB)	22.27° N	114.21° E	1954	2016
Tai Po Kau (TPK)	22.42° N	114.19° E	1963	2016
Tsim Bei Tusi (TBT)	22.48° N	114.02° E	1974	2016
Chi Ma Wan (CMW)	22.22° N	114.00° E	1963	1997
Cheung Chau (CHC)	22.19° N	114.03° E	2004	2016
Lok On Pai (LOP)	22.35° N	114.00° E	1981	1999
Ma Wan (MW)	22.35° N	114.06° E	2004	2016
Tai Miu Wan (TMW)	22.26° N	114.29° E	1996	2016
Shek Pik (SP)	22.21° N	113.89° E	1999	2016
Waglan Island (WAG)	22.17° N	114.30° E	1995	2016
Ko Lau Wan (KLW)	22.45° N	114.34° E	2004	2016
Kwai Chung (KC)	22.31° N	114.12° E	2004	2016
Dongfang (DF)	19.10° N	108.62° E	1975	1997
Beihei (BH)	21.48° N	109.08° E	1975	1997
Haikou (HK)	20.02° N	110.28° E	1976	1997
Zhapo (ZP)	21.58° N	111.83° E	1975	1997
Shanwei (SW)	22.75° N	115.35° E	1975	1997
Xiamen (XM)	24.45° N	118.07° E	1954	1997
Keelung (KL)	22.62° N	120.29° E	1980	2014
Kaohsiung (KS)	25.16° N	121.75° E	1980	2014
Manila, PHL (MN)	14.59° N	120.97° E	1984	2016
Vung Tau, VTM (VT)	10.34° N	107.07° E	1986	2014*
Sedili, MLY (SD)	1.93° N	104.12° E	1986	2016
Bintulu, MLY (BT)	3.22° N	113.07° E	1992	2016
Ishigaki, JPN (IG)	24.33° N	124.15° E	1968	2013

*-missing data from 2002-2007

Table 2 Amplitude TACs for M_2, S_2, K_1, and O_1. All values given are in units of milimeter change in tidal amplitude for a 1-meter fluctuation in sea level (mm m^{-1}). Statistically significant positive values are given in bold italic text.

Station	**M_2 TAC**	**S_2 TAC**	**K_1 TAC**	**O_1 TAC**
Quarry Bay (QB)	***+218 ± 37***	***+85 ± 16***	***+220 ± 15***	***+146 ± 11***
Tai Po Kau (TPK)	***+267 ± 42***	***+98 ± 17***	***+190 ± 68***	***+100 ± 25***
Tsim Bei Tusi (TBT)	+7 ± 80	-10 ± 15	+32 ± 22	+24 ± 22
Chi Ma Wan (CMW)	***-58 ± 11***	-7 ± 5	-18 ± 8	***-37 ± 10***
Cheung Chau (CHC)	***-63 ± 20***	-22 ± 35	***+69 ± 48***	+50 ± 92
Lok On Pai (LOP)	***-81 ± 24***	-18 ± 8	+8 ± 32	-24 ± 12
Ma Wan (MW)	***-68 ± 4***	+1 ± 25	***+52 ± 4***	***-62 ± 21***
Tai Miu Wan (TMW)	+22 ± 59	-1 ± 9	+10 ± 22	+3 ± 8
Shek Pik (SP)	***+62 ± 29***	+11 ± 18	***+70 ± 4***	+28 ± 17
Waglan Island (WAG)	+1 ± 21	+3 ± 6	+9 ± 7	-9 ± 8
Ko Lau Wan (KLW)	-46 ± 39	-11 ± 17	+29 ± 65	+60 ± 57
Kwai Chung (KC)	-90 ± 46	-10 ± 29	-91 ± 226	***-202 ± 161***
Dongfang (DF)	***+190 ± 75***	***+43 ± 9***	***+482 ± 53***	***+320 ± 52***
Beihei (BH)	***+461 ± 170***	***+88 ± 19***	***+579 ± 152***	***+294 ± 78***
Haikou (HK)	***+379 ± 106***	***+55 ± 8***	***+180 ± 28***	***+194 ± 37***
Zhapo (ZP)	-32 ± 30	-12 ± 30	+40 ± 33	+1 ± 44
Shanwei (SW)	+30 ± 30	-34 ± 31	-26 ± 15	***-79 ± 53***
Xiamen (XM)	+93 ± 31	-32 ± 35	***-46 ± 4***	***-48 ± 8***
Keelung (KL)	***-69 ± 14***	***-37 ± 5***	-4 ± 8	***+21 ± 4***
Kaohsiung (KS)	+25 ± 8	+1 ± 18	+1 ± 8	+28 ± 16
Manila, PHL (MN)	-17 ± 16	***-21 ± 9***	***+83 ± 12***	-20 ± 16
Vung Tau, VTM (VT)	+21 ± 26	***-44 ± 7***	+7 ± 21	+20 ± 6
Sedili, MLY (SD)	***-72 ± 35***	+24 ± 24	***-148 ± 35***	-54 ± 33
Bintulu, MLY (BT)	-37 ± 15	+11 ± 7	***+291 ± 45***	***+320 ± 36***
Ishigaki, JPN (IG)	***-46 ± 2***	-8 ± 7	***+23 ± 11***	+1 ± 11

Table 3 The δ-HAT$_4$, δ-HAT$_8$, D_1/D_2 TACs, and OT TACs. The δ-HAT values given are in units of milimeter change in tidal amplitude for a 1-meter fluctuation in sea-level (mm m^{-1}). D_1/D_2 and OT TACs are in unitless ratios (i.e., mm mm^{-1}) Statistically significant positive values are given in bold italic text.

Station	**δ-HAT$_4$**	**δ-HAT$_8$**	**D_1/D_2**	**OT/ (D_1 + D_2)**
Quarry Bay (QB)	***+665 ± 82***	***+834 ± 108***	***+1.08 ± 0.05***	***-3.62 ± 0.99***
Tai Po Kau (TPK)	***+612 ± 210***	***+797 ± 138***	***+1.01 ± 0.04***	***-1.87 ± 0.10***
Tsim Bei Tusi (TBT)	+56 ± 117	+41 ± 180	***+0.37 ± 0.02***	***-1.69 ± 0.14***
Chi Ma Wan (CMW)	***-119 ± 19***	***-159 ± 28***	***+0.74 ± 0.19***	-0.01 ± 0.60
Cheung Chau (CHC)	-12 ± 42	+224 ± 646	+0.81 ± 1.03	-0.11 ± 1.36
Lok On Pai (LOP)	-114 ± 45	-112 ± 110	***+0.26 ± 0.05***	-0.26 ± 0.21
Ma Wan (MW)	***-91 ± 73***	***-117 ± 35***	+0.57 ± 1.02	-0.42 ± 1.44
Tai Miu Wan (TMW)	+42 ± 100	+89 ± 99	***+1.04 ± 0.20***	***-1.31 ± 0.23***
Shek Pik (SP)	***+138 ± 37***	***+183 ± 20***	***+0.89 ± 0.06***	-0.01 ± 0.60
Waglan Island (WAG)	+3 ± 31	+4 ± 30	***+1.11 ± 0.17***	***-3.05 ± 0.43***
Ko Lau Wan (KLW)	-66 ± 47	+83 ± 367	***+1.31 ± 0.62***	-0.35 ± 0.82
Kwai Chung (KC)	-55 ± 64	+270 ± 730	***+1.19 ± 0.60***	***-0.62 ± 0.42***
Dongfang (DF)	***+1037 ± 453***	***+1236 ± 113***	***+2.86 ± 0.19***	***-6.10 ± 2.69***
Beihei (BH)	***+1405 ± 453***	***+2190 ± 151***	***+1.22 ± 0.03***	***-5.21 ± 0.15***
Haikou (HK)	***+813 ± 217***	***+1086 ± 189***	***+0.61 ± 0.05***	***-1.75 ± 0.04***
Zhapo (ZP)	-34 ± 111	-16 ± 69	+0.14 ± 0.07	***-1.69 ± 0.57***
Shanwei (SW)	-94 ± 94	***-217 ± 150***	+0.02 ± 0.18	-0.09 ± 0.20
Xiamen (XM)	+54 ± 38	-3 ± 43	***+0.12 ± 0.04***	***-0.92 ± 0.23***
Keelung (KL)	***-95 ± 21***	***-125 ± 44***	+0.08 ± 0.11	***-1.29 ± 0.57***
Kaohsiung (KS)	+54 ± 36	+52 ± 83	+0.16 ± 0.07	-1.55 ± 0.74
Manila, PHL (MN)	+39 ± 67	+5 ± 53	***+0.81 ± 0.61***	***-1.86 ± 0.49***
Vung Tau, VTM (VT)	-28 ± 22	-11 ± 59	+0.15 ± 0.08	+0.40 ± 0.59
Sedili, MLY (SD)	***-254 ± 70***	-76 ± 55	***-0.63 ± 0.06***	***-1.33 ± 0.50***
Bintulu, MLY (BT)	***+600 ± 52***	***+942 ± 55***	***-3.81 ± 1.60***	+1.62 ± 0.98
Ishigaki, JPN (IG)	***-58 ± 6***	+4 ± 24	***-0.12 ± 0.09***	+0.31 ± 0.61

Table 4 Correlations of tidal components with the North Point/Quarry Bay (QB) tide gauge, showing M_2, K_1, N_2, $2N_2$, M_3, and MO_3. Two numbers are given in each column, representing the correlations in the "historical" era (pre-1997), and the "modern" era (post-1997). Non-existent data is indicated by "~". An average value is also calculated at the local (Hong Kong) and regional (South China Sea) scale for each era. Data records that cover both time periods will indicate the better correlated era by bold text. Other tidal component correlations (including MSL) are given in Table S3 in the supplementary material.

Station	M_2	K_1	N_2	$2N_2$	M_3	MO_3
TPK	**0.83**/0.56	**0.72**/0.30	**0.71**/0.57	0.54/**0.73**	0.76/**0.77**	0.74/**0.78**
TBT	0.58/**0.77**	**0.48**/0.19	0.72/**0.78**	0.48/**0.70**	0.45/**0.52**	0.66/**0.78**
CMW/CHC	0.49/**0.56**	**0.42**/0.21	**0.69**/0.61	0.61/**0.94**	**0.88**/0.80	**0.92**/0.90
LOP/MW	**0.57**/0.11	**0.55**/0.16	**0.87**/0.76	0.74/**0.95**	**0.85**/0.29	**0.88**/0.87
TMW	~/0.25	~/0.60	~/0.65	~/0.87	~/0.76	~/0.93
SP	~/0.30	~/0.56	~/0.59	~/0.83	~/0.59	~/0.83
WAG	~/0.22	~/0.52	~/0.62	~/0.82	~/0.76	~/0.90
KC	~/0.20	~/0.25	~/0.76	~/0.93	~/0.82	~/0.92
KLW	~/0.16	~/-0.02	~/0.70	~/0.92	~/0.76	~/0.94
HK Ave.	**0.62**/0.28	**0.54**/0.31	**0.75**/0.67	0.59/**0.86**	**0.74**/0.67	0.80/**0.88**
DF	0.78/~	0.62/~	0.63/~	0.63/~	-0.32/~	-0.27/~
BH	0.75/~	0.58/~	0.55/~	0.35/~	-0.03/~	0.13/~
HK	0.82/~	0.53/~	0.61/~	0.27/~	0.18/~	0.21/~
ZP	0.34/~	0.68/~	0.78/~	0.12/~	0.75/~	0.64/~
SW	0.73/~	0.32/~	0.83/~	0.77/~	0.84/~	0.89/~
XM	-0.49/~	0.24/~	0.61/~	-0.47/~	-0.63/~	-0.15/~
KL	~/-0.32	~/-0.13	~/0.49	~/0.18	~/0.45	~/-0.37
KS	~/0.34	~/0.62	~/0.53	~/0.53	~/0.14	~/-0.10
MN	~/-0.16	~/-0.07	~/0.06	~/0.50	~/0.48	~/0.35
VT	~/0.49	~/0.63	~/0.56	~/0.08	~/0.54	~/-0.03
SD	~/0.40	~/-0.46	~/0.80	~/0.79	~/-0.03	~/-0.31
BT	~/0.10	~/0.54	~/0.19	~/0.21	~/0.19	~/-0.17
IG	0.18/**0.36**	**0.38**/0.07	0.62/**0.72**	0.34/**0.54**	**0.52**/0.47	-0.17/**0.08**
SCS Ave.	**0.45**/0.17	**0.48**/0.17	**0.66**/0.48	0.29/**0.41**	0.19/**0.32**	**0.12**/-0.09